

Controlled heavy haul traffic loading as a method to remediate liquefiable soft silts

Krechowiecki-Shaw, Christopher; Royal, Alexander; Jefferson, Ian

DOI:
[10.1139/cgj-2017-0223](https://doi.org/10.1139/cgj-2017-0223)

License:
None: All rights reserved

Document Version
Peer reviewed version

Citation for published version (Harvard):
Krechowiecki-Shaw, C, Royal, A & Jefferson, I 2019, 'Controlled heavy haul traffic loading as a method to remediate liquefiable soft silts', *Canadian Geotechnical Journal*, vol. 56, no. 7, pp. 911-928.
<https://doi.org/10.1139/cgj-2017-0223>

[Link to publication on Research at Birmingham portal](#)

Publisher Rights Statement:

Final version of record to appear in Canadian Geotechnical Journal - <http://www.nrcresearchpress.com/journal/cgj>

General rights

Unless a licence is specified above, all rights (including copyright and moral rights) in this document are retained by the authors and/or the copyright holders. The express permission of the copyright holder must be obtained for any use of this material other than for purposes permitted by law.

- Users may freely distribute the URL that is used to identify this publication.
- Users may download and/or print one copy of the publication from the University of Birmingham research portal for the purpose of private study or non-commercial research.
- User may use extracts from the document in line with the concept of 'fair dealing' under the Copyright, Designs and Patents Act 1988 (?)
- Users may not further distribute the material nor use it for the purposes of commercial gain.

Where a licence is displayed above, please note the terms and conditions of the licence govern your use of this document.

When citing, please reference the published version.

Take down policy

While the University of Birmingham exercises care and attention in making items available there are rare occasions when an item has been uploaded in error or has been deemed to be commercially or otherwise sensitive.

If you believe that this is the case for this document, please contact UBIRA@lists.bham.ac.uk providing details and we will remove access to the work immediately and investigate.

**--Controlled heavy haul traffic loading as a method to
remediate liquefiable soft silts**

C. J. Krechowiecki-Shaw, A. C. D. Royal, I. Jefferson

C. J. Krechowiecki-Shaw. Arup, 560 Mission Street, Suite 700, San Francisco, CA 94105, USA.

Christopher.Shaw@arup.com

Dr. A. C. D. Royal. University of Birmingham School of Engineering, Edgbaston, Birmingham, B15

2TT. A.C.Royal@bham.ac.uk

Prof. I. Jefferson. University of Birmingham School of Engineering, Edgbaston, Birmingham, B15

2TT. I.Jefferson@bham.ac.uk

Abstract

Transportation of extremely large indivisible loads (10,000 to 30,000 tonnes) is becoming increasingly popular to allow offsite modular construction of infrastructure for oil and gas, mining and renewable energy projects in remote areas. Such exceptionally large transient loads could encounter unusual geohazards; there is a risk of metastable liquefaction when crossing soft alluvium, causing sudden failure, potential casualties and severe production delays. Furthermore, temporary roads for these payloads are a large cost to such projects; conventionally designed earthworks and/or ground improvement is often unaffordable or logistically impossible.

This laboratory study indicates the fabric can be strengthened, and the hazard reduced, if the soil is subject to careful repeated loading which rearranges the initially precarious fabric through gradual accumulation of plastic strains. A novel remediation technique for these temporary haul roads is proposed; managed deployment of increasingly heavy haul vehicles could result in staged fabric rearrangement that strengthens the soil to the point where it would be safe for the heavy vehicles to use it. In so doing, a more economic temporary haul road is open to operations (coupled with observation methods to ensure adequate performance throughout) and production activities are not overly disrupted.

Keywords: cyclic loading, liquefaction, temporary roads, metastable soil

32 **List of symbols:**

- 33 A – sample representative cross-sectional area (mm^2)
- 34 A_0 – initial sample A prior to consolidation (mm^2)
- 35 A_c – sample A following anisotropic consolidation (mm^2)
- 36 e – void ratio (dimensionless)
- 37 e_0 – initial void ratio prior to consolidation (dimensionless)
- 38 e_c – void ratio after final, anisotropic consolidation stage (dimensionless)
- 39 K – coefficient of lateral earth pressure (dimensionless)
- 40 $K_{0,NC}$ – normally consolidated coefficient of lateral earth pressure at rest (dimensionless)
- 41 N – number of cycles (dimensionless)
- 42 OCR – overconsolidation ratio (dimensionless)
- 43 p' – mean normal effective stress (kPa)
- 44 PI – Plasticity Index (%) ($= LL - PL$)
- 45 PL – Plastic Limit as per BS 1377-2 (BSI, 1990a) (%)
- 46 q – deviator stress (kPa)
- 47 q_{max} – deviator stress at cycle maximum (kPa)
- 48 q_{min} – deviator stress at cycle minimum (kPa)
- 49 q_{peak} – pre-liquefaction peak (monotonic) deviator stress (kPa)
- 50 Δq – increment in deviator stress from start of shear stage (kPa)
- 51 Δq_{cyc} – peak cyclic deviator stress range (kPa) $= q_{max} - q_{min}$
- 52 Δq_{peak} – increment in deviator stress from start of (monotonic) shear to pre-liquefaction peak (kPa)
- 53 Δq_{ult} – increment to ultimate deviator stress from start of (monotonic) shear (kPa)
- 54 u – sample pore water pressure (kPa)
- 55 u_e – excess pore water pressure (kPa)
- 56 u_{max} – maximum value of u attained in a particular cycle (kPa)
- 57 u_{pl} – irrecoverable (plastic) value of u attained at the end of a particular cycle (kPa)
- 58 Δu_{pl} – increment of irrecoverable (plastic) value of u attained in a particular cycle (kPa)
- 59 ε – axial strain (dimensionless)
- 60 ε_{max} – maximum axial strain experienced in a particular cycle (dimensionless)

- 61 ε_{pl} – cumulative plastic axial strain in a particular cycle (dimensionless)
- 62 $\Delta\varepsilon_{cyc}$ – cyclic strain range for a particular cycle (dimensionless)
- 63 $\Delta\varepsilon_{el}$ – recoverable (elastic) axial strain in a particular cycle (dimensionless)
- 64 $\Delta\varepsilon_{pl}$ – increment in plastic axial strain in a particular cycle (dimensionless)
- 65 σ_1 – axial total stress (kPa)
- 66 σ'_3 – total confining stress (kPa)
- 67 σ'_1 – axial effective stress (kPa)
- 68 σ'_3 – confining effective stress (kPa)

69 **1. Introduction**

70 To avoid exposure of workers to remote, potentially inhospitable sites with associated logistical and
71 quality assurance difficulties, projects in the mining, power generation, oil and gas sectors often pre-
72 fabricate modular infrastructure off-site (Mammoet, 2017). Hence, very large indivisible loads, up to
73 3000 tonnes must be transported via temporary roads on large platforms with multiple axles (e.g. 80
74 axles arranged in 40 rows; Mammoet, 2017). After transportation, the roads may have no residual
75 value; the design and construction approach must therefore focus on minimising cost. Conversely,
76 very large loads necessitate robust road foundations for overall stability, particularly where roads
77 cross soft ground. Recent silty deposits (i.e. alluvium) present the additional unusual risk of
78 metastable liquefaction at depth to this heavy haul traffic. This is a result of interaction between
79 adjacent wheel stress bulbs stressing much deeper soil than conventional traffic (Krechowiecki-Shaw
80 et al., 2017), which can be normally consolidated and prone to liquefaction under relatively small
81 disturbances. This rapid and catastrophic failure mode could suddenly topple or strand a heavy haul
82 vehicle, with risk of casualties, irreparable damage to these multimillion-dollar payloads and
83 ultimately significant production delays.

84 An observation design approach, using in-situ monitoring data to infer behavioural changes in the
85 soil and inform remedial works where necessary, would permit more economical design, reduced

access costs and mitigate risks. This paper demonstrates that in certain conditions, where liquefiable deposits are present at relatively shallow depths (i.e. 6-10m), the action of traffic can improve the resistance of soft subgrade soil; observational design could thus be used to deliver ground improvement and thus substantially more reliable and affordable temporary infrastructure.

2. Initiating and averting metastable liquefaction

It was demonstrated by Krechowiecki-Shaw et al. (2017) that a heavy haul vehicle can apply transient stresses to soil at depth, in a normally consolidated state (e.g. at 6.5m depth for the very soft soil considered), with sufficient magnitude to induce localised plastic yield. Reaching yield in liquefiable silty deposits is of particular concern, as yield is strain-softening. Instead of mobilising an additional reserve of bearing resistance from perfect plasticity and stress redistribution (Osman and Boulton, 2005; Madabhushi and Haigh, 2015), resistance can be lost. After reaching a small initiation strain (in the order of 0.1% strain: Lade, 1994; Yamamuro and Lade, 1999; Wang et al., 2014) and with little prior warning, unlimited or very large ground movements can occur. For example, Sadrekarimi (2014) cites cases of flowslides of metastable silty sand slopes initiated by small disturbances (e.g. oversteepening, construction loads) which travelled up to 2000m.

Metastable liquefaction takes place under undrained conditions; liquefaction is impossible in drained conditions (Been and Jefferies, 1985; Lade, 1999). Plastic clays are more resistant to liquefaction due to their electro-chemical activity (Andrews and Martin, 2000). For slow-moving traffic loads, silts may present a worst-case liquefaction risk, being both sufficiently inactive to liquefy and insufficiently permeable to drain under load.

Metastable liquefaction is considered highly dependent upon a precarious initial fabric arrangement (Lade, 1999). Strain threshold terminology, following Díaz-Rodríguez and López-Molina (2008), is useful for describing the changing behaviour of a soil and progressive loss of influence of the initial fabric with strain due to restructuring (Figure 1). A liquefiable soil can be considered unique in that

medium-strain perturbations (small irreversible fabric rearrangement) can initiate large-strain flow (complete fabric re-structuring). Investigation of undrained granular assemblies using the Discrete Element Method (DEM) by Kruyt (2010) and Gu et al. (2014) suggest the way in which global shear resistance is mobilised changes with increasing plastic strain, from predominantly tangential interparticle forces at small strains to predominantly normal interparticle forces at large strains, with the soil skeleton rearranging to form a preferential arrangement in response to the load. This rearrangement also causes irreversible contraction (or dilation) of the assembly and loss (or gain) of contact points per particle. In very loose DEM assemblies investigated by Gong (2008), this loss of contact points can be such that static equilibrium is no longer maintained and is hypothesised to be the mechanism for liquefaction.

Edwards et al. (2004) theorised that, due to frictional restraint, particles in a granular assembly are only free to seek the lowest energy state (i.e. a denser packing) if sufficient agitation overcomes energy barriers. The medium-strain threshold represents this minimum agitation, whereby minimal numbers of particles are liberated. Under a larger mechanical energy input liquefaction is initiated; a far larger number of particles are simultaneously liberated, triggering a chain reaction of contact breakage which destabilises the soil skeleton. Metastable soils in this context may be characterised as having unusually large differential between the initial and lowest possible energy state. Clearly a loose initial packing is important to achieve this.

Contraction in undrained shear, characteristic of normally consolidated or lightly overconsolidated soil, is required to trigger this type of liquefaction (Been and Jefferies, 1985; Lade, 1999). Increasing overconsolidation ratio (OCR) from 1 to 2 is found to change static behaviour of Mississippi River Valley silt from liquefying to strain-hardening (Wang and Luna, 2012) and significantly increase cyclic resistance (Wang et al., 2016). Similar behaviour is seen in sand (Been and Jefferies, 1985) and low-plasticity clay (Santagata and Germaine, 2005) when a normally consolidated and overconsolidated response are compared. The reduced contraction in undrained shear and retention of lower void

ratio than an equivalent normally consolidated soil (after Schofield and Wroth, 1968) are expected to be responsible for this behavioural change.

Initiation of metastable liquefaction is governed by the soil's effective stress state, occurring when a certain ratio of shear to normal effective stress (i.e. q/p') is mobilised, termed the Instability Line (Lade, 1994). Whilst this Instability Line remains constant for soil prepared, consolidated and sheared without complex stress history (Lade, 1994; Doanh et al., 2012), applying a load-unload stress history can change the angle of the Instability Line to be preferentially stronger in one direction (Doanh et al., 2012). The Instability Line can therefore be considered a function of fabric and a property that can be changed through changes to fabric.

Post-cyclic monotonic tests (Ward, 1983; Togrol and Güler, 1984; Wang et al., 2015) indicate that raising pore water pressures through cyclic pre-loading results in similar monotonic shear response to samples overconsolidated by removal of the same external stress. Cyclic loading can reduce the post-cyclic monotonic strength if strains are high (Brown et al., 1977; Díaz-Rodríguez and Santamarina, 2001; Santagata and Germaine, 2005) but can also improve strength if plastic cyclic strains are sufficiently low (e.g. less than 3% in Brown et al., 1977; 0.5% in Santagata and Germaine, 2005). Whether this is primarily as a result of changes to the stress state or beneficial fabric rearrangement is unclear.

If a soil's in-situ fabric arrangement can be altered to make the arrangement less precarious or to change volumetric behaviour from contraction to dilation (i.e. behave as if overconsolidation has been induced), then it may be possible to treat a liquefiable soil through mechanical application of cyclic load. Developing a certain amount of irreversible fabric rearrangement is expected to be necessary to effect the necessary behavioural change in the soil skeleton. Silt cyclically loaded and then consolidated before monotonic shearing by Wang et al. (2014) demonstrated similar behaviour; unless the cyclic yield strain (determined after Erken and Ulker, 2007) was exceeded, no changes to strength from consolidation was observed. This paper presents results from triaxial

testing on a silt soil prepared in a metastable condition, which demonstrate medium-strain cyclic pre-loading can disrupt the metastable energy state and stabilise liquefiable soil without actually triggering liquefaction. Cyclic pre-loading, effected by carefully controlled traffic passages, could therefore use this mechanism to stabilise deep liquefiable soils beneath heavy haul roads and thus improve both economy and reliability of this temporary infrastructure.

3. Testing method

A series of cyclic and static triaxial tests were performed on a synthetic silt mix soil in order to investigate the trigger conditions for liquefaction, threshold stresses and strains (see Figure 1) and changes in behaviour induced by cyclic loading and plastic strain accumulation and so demonstrate how gradual strain accumulation through cyclic load can strengthen liquefiable soil.

3.1. Soil classification

The soil used in these experiments (referred to as 'Silt Mix' soil) is a blend of commercially available geomaterials, used to ensure consistency throughout the test programme, as follows:

- 25% (by mass) Blooma playpit sand (medium to fine, subangular to angular-grained silica sand, supplied by B&Q PLC)
- 60% Silverbond M10 Silica Flour (silt-sized ground silica, supplied by Minerals Marketing)
- 15% Puraflo 50 English China Clay (low activity Kaolinite clay, supplied by Potteryworks Ltd.)

When mixed to form a soil of soft consistency, it is liquefiable under repeated hand pressure and displays dilatancy when sheared by hand following procedures in BSI (2015). The Silt Mix had Liquid Limit (*LL*) of 21-22% (determined using the Drop-Cone method of BSI, 1990), a Plastic Limit (*PL*) of 14-15% and a Plasticity Index (*PI*) of 7-9%, corresponding to low-plasticity Clay just above the 'A-line' on a Casagrande Chart. Hydrometer tests indicate 8-12% of the Silt Mix is finer than 2 μ m. Particle density tests (BSI, 1990) indicate a relative density of 2.69 ± 0.03 .

The low LL and fraction finer than $2\mu\text{m}$, combined with the low activity expected from the silt minerals (recently crushed silica with no alteration), suggests the Silt Mix is likely to behave in a ‘granular’ manner (Andrews and Martin, 2000).

3.2. Specimen preparation

It is particularly important when preparing silty/sandy soils to note that the fabric generated during sample preparation, e.g. whether a sample is created by compaction of moist soil or consolidation from slurry, has an impact on the mechanical response (Bradshaw and Baxter, 2007). It is also important to reproduce a similar stress state to recent alluvial deposits, i.e. normally consolidated at reasonably low stresses. A slurry consolidation preparation technique was thus chosen, based on work by Wang et al. (2011), because:

- It is possible to produce a very soft sample by changing the consolidation load; reconsolidation to a normally consolidated state then requires only relatively low stresses
- Soil fabric is expected to be more representative of recent alluvial silt; a clear difference is apparent when compared to a soft sample produced by compaction (Figure 2)

Commonly, clay samples are consolidated to the desired water content from slurries mixed at a water content of 2 to 3 LL (e.g. Brown et al., 1975; O’Reilly et al., 1988; Lin and Penumadu, 2005). However for predominantly silty soils this carries a risk of fines segregation. Following Wang et al. (2011), the Silt Mix slurry was mixed at 1.5 LL ; this was found to be sufficiently fluid to not hold open air bubbles but thick enough to resist segregation.

Friction between the slurry mould and slurry can produce samples of non-uniform water content. Valls-Marquez et al. (2008) found lenses of wet, soft soil after consolidating clay from slurry: water contents at mid-height could be 8% higher than the ends. Intra-sample variations of this magnitude introduce difficulty in analysis; selecting a uniform water content to represent sample behaviour is unrealistic. Furthermore, due to the Silt Mix’s low PI , water content differences of over 3% between

ends and mid-height resulted in the sample slumping in the middle under its own weight, even though the top of the sample was stiff.

Changes were made based upon the silt slurry consolidation method developed by Wang et al. (2011), which achieved a maximum water content difference of 1.2%. A latex membrane containing the soil slurry reduced friction and intra-sample water content differences. The membrane also restrained the sample upon mould extraction and reduces slumping tendencies. For maximum effect, the latex membrane needed to also enclose the top cap, otherwise a small quantity of slurry can become trapped against the mould and provide increasing frictional resistance as the cap settles. With these changes to mould design, consistency was improved to typically maintain water content differences of below 1.5%, sufficient to resist necessary handling to set up triaxial tests without slumping. The impact of various sleeving arrangements is shown in Figure 3. Moisture contents at this stage were estimated (from consolidation volume change measurement) to be 20-21%, i.e. void ratio, $e = 0.54$ to 0.56 .

Following Wang et al. (2011), the procedure minimised handling of the soft samples, thus minimising disturbance. To avoid transporting, samples were consolidated on the triaxial cell platen using the ram. A split mould, cut from a 100mm diameter PVC pipe, was used so the top cap could be fitted and sealed before the mould was removed. Even with these precautions, some samples were disturbed during test set-up and slumped, resulting in significant changes in to observed behaviour (see Section 4.5).

Once extracted from the mould, samples were consolidated anisotropically to reflect at-rest conditions at depth in a young deposit. The deviator stress applied during consolidation is also expected to increase risk of liquefaction, as the stress increment required to reach the Instability Line is reduced (Doanh et al., 2012). No backpressure saturation stages were needed as all samples achieved a B value of 0.95 or greater. During consolidation, a backpressure of 100kPa was maintained such that negative excess pressures could be tolerated without cavitation (Head, 1986).

The normally consolidated lateral earth pressure coefficient at rest ($K_{0,NC}$) was determined by consolidating samples by matching the axial strain to the volume change to maintain a constant area, as described in Head (1986), and a value of $K = 0.45$ found. For expediency of the testing program, most tests were consolidated anisotropically to this stress state through two stages; an initial isotropic stage to achieve the desired effective confining pressure, followed by a gradual increase in deviator stress. Undrained static tests consolidated in this manner were found to be acceptably similar to those consolidated under explicit zero lateral strain conditions, i.e. both produced liquefaction at 0.1% to 0.3% strain following a deviator stress increment of 23-29kPa and recovery after 1.5% to 3% strain.

To achieve a comparable stress state between the overconsolidated samples sheared monotonically and post-cyclic monotonic shear tests, two samples were overconsolidated from their anisotropic normally consolidated state by lowering the cell pressure, to simulate loss of effective stress through rising pore pressure.

Static and cyclic testing was performed using the VJTech Dynamic Triaxial Testing System (DTTS). Pore water pressure was measured by a base transducer, axial load by a submersible load cell and cell and back pressures were controlled by pneumatic and hydraulic Automatic Pressure Controllers respectively, the latter also allowing measurement of volume change during consolidation.

A unique identifier was assigned to each sample tested in order to catalogue the varying test conditions. They denote the test series (M for monotonic tests, CA/CB/CC for cyclic test series A, B, C). For cyclic tests, additional information is provided in a second number denoting the cyclic loading relative the liquefaction threshold (i.e. 154 indicates $\Delta q_{cyc}/\Delta q_{peak} = 1.54$) and a third number relating either to repeated test conditions (e.g. CA-154-2 is the second repeat test) or in the case of series C tests with variable cycle counts, the number of cycles (i.e. CC-154-7 has 7no. cycles of $\Delta q_{cyc}/\Delta q_{peak} = 1.54$).

Frictional restraint of the triaxial sample ends prevents radial expansion and results in non-uniform stress distribution through the sample (Bishop and Green, 1965; Sheng et al., 1997) which has been found to reduce the failure strain (Schofield and Wroth, 1968, Lee, 1978) and increase strain under cyclic load (Lee and Vernese, 1978). Placing a lubricated membrane and disc assembly beneath the sample (following Head, 1986) was not possible without lifting and disturbing the soft sample. However it was possible to place a lubricated end assembly on top of the sample, thus doubling its effective length with respect to end restraint (similarly to Kirkpatrick and Belshaw, 1968). A few tests were conducted in this manner to investigate end restraint effects, but as the inclusion of compressible grease tends to obfuscate the true stiffness behaviour at low strains (i.e. close to those at which liquefaction occurs) the majority were tested without.

3.3. Strain thresholds

Understanding the medium-strain threshold (i.e. initiation of plasticity) is important to determine the extent to which cyclic load rearranges the soil fabric, and to inform selection of appropriate cyclic stresses. The test method of Hsu and Vucetic (2006) uses Direct Simple Shear apparatus to determine this threshold with servo-controlled vertical stress to maintain constant volume conditions (and thus records a very accurate pore pressure response). Strain-controlled cycles of increasing magnitude are applied until external indications of plasticity (i.e. accumulation of pore pressure) are observed; this marks the medium-strain threshold. Triaxial apparatus with measurement of pore pressures in the base cannot perform this test with the same accuracy; lower strains at the radially-restrained base reduce the tendency to contract (Bishop and Green, 1965) and the medium-strain threshold may thus be overestimated. However measurement of deviator stress (for anisotropically consolidated samples) under strain-controlled cycles shows an initiation of cyclically-induced relaxation (Figure 4). This implies that initiation of plastic behaviour is not properly detected by the base pore pressure transducer: global sample axial stress appears to be a more useful indicator of medium-strain behaviour. This apparent medium-strain threshold between 0.01%

and 0.025% is in agreement with results for low plasticity silts and clays presented by Díaz-Rodríguez and López-Molina (2008).

3.4. Area corrections

During loading, correction of the sample area with strain for estimation of a representative global stress is required. The conventional volume equivalent right cylinder method is used in this study:

Equation 1:

$$[1] \quad A_c = A_0 \frac{1 - \frac{\Delta V}{V_0}}{1 - \frac{\varepsilon_a}{100\%}}$$

Results from Sheng et al. (1997) show this correction to be acceptably similar to more sophisticated methods (which use local measurements) up to around 10-15% strain for a ‘barreling’ sample with frictional end restraint and hence is considered acceptable for use in this study.

In order to respond to feedback in cyclic tests sufficiently quickly, the DTTS’s cyclic control algorithms are based on either ram displacement or axial load measurement (i.e. not stress directly). During undrained, load-controlled cyclic tests, the cyclic and permanent (from anisotropic consolidation) components of the deviator stress reduce with increasing strain (due to increasing sample area; Equation 1). Relaxation of deviator stress is particularly significant (Figure 5); when the maximum and minimum cyclic stress is maintained constant by manually adjusting the cyclic load range (in line with Equation 1) strain accumulation is significantly increased, as can be observed when comparing cyclic series A (CA, uncorrected) and B (CB, corrected) tests. In fact, a previously stable cyclic test (25kPa, CA-96) liquefies if this correction is included (as in test CB-96-1); neglecting this correction overestimates the threshold stress.

3.5. Interaction with creep

Creep strains are strains that continue after excess pore water pressures have dissipated and during the subsequent shear stages. For undrained monotonic tests, Santagata and Germaine (2005)

suggested the strain rate should be 30 to 50 times faster than the final consolidation creep rate to avoid creep influencing the test. Typically, final consolidation creep rates were found to be 0.005%/hr to 0.01%/hr; the strain rate used in monotonic tests, 1.3%/hr, is sufficiently fast to avoid such interaction and still develop representative base pore water pressure readings before failure (Head, 1986; BSI, 1990).

Tests CB-31-1, CB-31-2 and CB-31/77 experienced the smallest cyclic strains (i.e. 0.008%/cycle), remaining within the elastic strain region but at sufficiently fast rates to avoid interaction (equivalent to 0.43%/hr). However plastic strains still accumulated in these tests, at rates slightly faster than the recorded creep rates at the end of consolidation (i.e. 2.7 to 3.5 times faster). This is reduced but not eliminated by extending consolidation times (Figure 6). Pore pressure accumulation is also highly dependent upon creep rates. Given the elastic nature of these strains and strong dependence upon creep rates, it is likely they accumulate strain and pore pressure entirely as a result of creep interaction. Laboratory estimates of strain accumulation under such low loads are therefore likely to be significantly overestimated.

Tests CB-77 and the second part of CB-31/77 experienced an initial cyclic strain of 0.022% to 0.026% (i.e. close to the volume change threshold strain), but become similarly influenced by creep rates later in the test as the plastic axial strain increment per cycle, $\Delta\epsilon_{pl}$, reduces (Figure 7). Test CB-77, with the higher creep rate, reaches a near-constant plastic strain rate suggesting creep interaction. Whilst the limit from Santagata and Germaine (2005) appears effective in describing the range over which creep interaction is negligible, the similarity of the two tests up to cyclic plastic strains of 0.004% (i.e. 13 times the faster creep rate) suggest it may be conservative in this case.

3.6. Summary of triaxial tests

In order to simulate the 'deep' stress state considered of critical importance in Krechowicki-Shaw et al. (2017), anisotropically consolidated triaxial samples were subject to undrained cyclic deviator stress pulses of varying magnitude (except when close to failure, Krechowicki-Shaw et al., (2017),

found that these large vehicles did not induce significant principal stress rotation at depth). Monotonic undrained tests on normally consolidated samples were used to inform selection of cyclic stress levels. Cyclic loads close to the increment in deviator stress required to initiate static liquefaction (Δq_{peak}) were then applied and the effects of increasing or decreasing cyclic stresses on cyclic strain accumulation and instability were observed. After cyclic tests (unless cyclic strains were too large), a post-cyclic monotonic undrained shear stage was included to determine whether the cyclic load had improved or weakened the soil.

Testing conditions and outcomes are summarised in Tables 1 to 5. 'Intact' monotonic tests (i.e. sheared from anisotropic normal consolidation) are summarised in Table 1, overconsolidated tests in Table 2, cyclic series A, B and C tests are summarised in Tables 3, 4 and 5 respectively. 'L' in the test name indicates a lubricated top assembly was used (other samples have 'standard ends'), whilst 'd' indicates this sample is suspected to have been disturbed in preparation.

Note that the cyclic stress in tests is also normalised by the mean Δq_{peak} (26kPa), as further discussed in Section 4.1. All cyclic tests use haversine waveforms of frequency 0.01Hz unless stated otherwise. Figure 8 demonstrates the definitions of various cyclic stress, strain and pore pressure terms used frequently in analysis.

4. Experimental results

4.1. Cyclic and static liquefaction

Undrained shearing behaviour has strong connections to strain levels. Between strains of 0.1% and 0.3%, strain-softening liquefaction (loss of static stress or increasing cyclic plastic strain rates) is initiated in both monotonic and cyclic tests (Figure 9). Liquefaction is initiated at a consistent q/p' , i.e. the Instability Line (Figure 10). Liquefaction is temporary; strength recovers after sufficient strain (1.5% to 3.0%) and in monotonic tests a clear dilation during this recovery phase (over 4% strain) is apparent (Figure 9, Figure 10). Increasing post-liquefaction cyclic resistance also appears to mobilise

dilation, illustrating a change from pore water pressure response ‘lagging’ the stress pulse (as expected when finite sample permeability is considered) to ‘leading’ the stress pulse, i.e. the maximum cycle stress appears to induce a reduction in pore water pressure (Figure 11). A similar phenomenon of liquefaction at around 0.5% strain, followed by dilatant recovery, was previously observed in monotonic undrained tests by Wang et al. (2011, 2014) on natural Mississippi River Valley Silt.

Conventionally, the critical state strength of a soil is a sensible reference point for analysis (e.g. Andersen, 1988; Frost, 2000). However, as a critical state was not observed in this study (discussed further in Section 4.2), the mean pre-liquefaction peak in monotonic undrained shear is instead chosen to normalise cyclic stresses (i.e. $\Delta q_{cyc}/\Delta q_{peak}$); this has the additional advantage that it focuses analysis on the phenomenon of interest, i.e. metastable liquefaction.

Figure 9 indicates a cyclic ‘threshold stress’ between 0.77 and 0.96 Δq_{peak} (i.e. $\Delta \varepsilon_{pl}$ continually reduces in the former but not the latter): cyclic and monotonic liquefaction thus occur under similar stress increments. Under cyclic load, stability can be maintained for a limited number of cycles above the threshold stress (e.g. tests CB-96-1 and CB-154 in Figure 9). Liquefaction is triggered only when the initiation strain (strongly linked to pore water pressure and thus the Instability Line condition) and threshold stress are exceeded simultaneously. This is corroborated by test CA-96; gradual stress relaxation from above to below the threshold stress results in stability being maintained whilst the liquefaction initiation strain is exceeded (a final strain of 1.74%; Figure 5).

In agreement with results from Wang et al. (2014) and Santagata and Germaine (2005), overconsolidated samples no longer liquefy (Figure 12), although their ultimate strength is similar (due to the low swell potential of silt). At the lower OCR tested (1.1; test M-10), behaviour is continuously strain-hardening but the influence of the formerly precarious fabric is still apparent through loss of stiffness between 0.1% and 2.0% strain. Figure 13 shows the effective stress state of

both overconsolidated samples to have crossed the Instability Line during drained swell-back (i.e. stable conditions) and this may be responsible for subsequent stable behaviour.

Once unloaded from their insitu state, it has been observed that normally consolidated soil samples will retain some 'memory' of overconsolidation when reloaded to the previous stress state and require additional load (i.e. 1.5 to 4 times the previous maximum: Ladd and Foott, 1977; Overy, 1982; Santagata and Germaine, 2005) to regain normally consolidated behaviour. The cyclic response of a sample with such a stress history (i.e. taken to anisotropic normal consolidation, deviator stress then removed and reapplied) accumulates significantly less strain, as shown in Figure 14. The small apparent level of overconsolidation induced is sufficient to stabilise the fabric and avoid liquefaction even though final stress conditions the same.

4.2. Ultimate failure states

Whilst potentially catastrophic for heavy haul road traffic, meta-stable liquefaction is not an ultimate failure mode (Muhunthan and Worthen, 2011) and recovery of strength can follow. After liquefying, undrained effective stress paths of silt samples can show pore pressure dilation (e.g. Figure 10; Yamamuro and Lade, 1999; Wang and Luna, 2012). Silts able to withstand large strains and significant dilation can reach a plastic critical state with constant pore pressure and deviator stress (at strains over 20% in Yamamuro and Lade, 1999, and Wang and Luna, 2012). However this is not the only ultimate failure mode available; dilatant soil may not experience uniform dilation but may fail before the critical state through strain localisation, which is conversely brittle and strain-softening (Schofield and Wroth, 1968; Nova, 2010) and thus of greater concern to the haul road designer.

The tests presented herein all failed prematurely during dilation (at 7-11% with standard ends, 15% with lubricated top) through shear banding, after which behaviour is consistently strain-softening (once corrected for membrane restraint, following Head, 1986 and La Rochelle et al., 1988). This is relatively common (e.g. Ward, 1983) and is expected to be due to non-uniformity, either in

composition or stress field (from end platen roughness), which will accelerate a strain localisation (Nova, 2010). During the dilatant phase, lubricated samples were able to withstand greater strains (Figure 12) and hence achieve higher ultimate strengths, particularly following cyclic loading. Cyclic tests with lubricated ends also accumulated strain more slowly, particularly at large strains (Figure 15). Observed changes in the failure mode suggest this is due to more uniform stress conditions; instead of failing either in a single diagonal shear band or a double 'X' shaped mechanism, they exhibited a multi-planar, general shear failure (similarly observed by Lunne et al., 2006) implying increased ability to mobilise dilatant strength.

As the insitu stress field is likely to be highly non-uniform, designers should exercise caution when relying upon dilatant strengths. However, the transient nature of traffic loads does imply a lower risk of shear banding when compared to static load; micro-drainage across the discontinuity, which weakens the shear band locally, has less time to take place (Atkinson, 2000). This is supported by the failure modes of tests presented herein: all standard-end monotonic tests reached shear band failure at 7-11% strain but under similar cumulative strains, standard-end cyclic tests (excepting the most heavily loaded; $\Delta q_{cyc}/\Delta q_{peak} = 1.92$) remained stable and only failed in subsequent monotonic shear (Figure 16). Similarly, the ability of lubricated-end tests to withstand greater strains before shear banding is also apparent in these post-cyclic monotonic tests, but may not reflect the risk of premature insitu strain localisation failure.

Zhang & Garga (1997), testing uniform sands under undrained conditions, found the apparent recovery of strength after liquefaction predominantly arises from large-strain triaxial end restraint: lubricating sample ends reduced post-liquefaction recovery to near-negligible levels. Tests presented herein differ from Zhang and Garga (1997) in this respect; Silt Mix samples start to recover strength at much lower strains (1.5 to 3.0%), instead of large (10 to 20%) strains, when end restraint is expected to be significant (Bishop and Green, 1965; Sheng et al., 1997). Stress-strain response and cyclic strain accumulation only appears influenced by end restraint (i.e. lubricated and standard-

ended tests diverge) at very large strains (Figure 12; Figure 16). This greater propensity for dilatant recovery at lower strains may be a function of the soil used, viz. angular, more multi-graded silt.

4.3. Behaviour changes from cyclic pre-loading

If cyclic loading is sufficient to trigger liquefaction, the response to subsequent monotonic loading is much more dilatant and brittle than the monotonic response of intact (i.e. no cyclic stage) samples (Figure 16), implying induced overconsolidation similar to that observed by Ward (1983), Togrol and Güler (1984) and Li et al. (2011). It is apparent that the sum of cyclic plastic and monotonic strains governs shear band initiation; dilating soil requires large localised grain movements (i.e. large strains) to 'open up' a shear band (Atkinson, 2000, Zhao and Guo, 2015). Cyclically liquefied samples also have a tendency to fail at lower cumulative strains in shear banding during monotonic loading than intact tests (Figure 16). Large cumulative strains and pore water pressures can thus weaken soil and adversely alter the failure mode, which will compromise the ability of the haul road to resist subsequent heavy loads. In agreement with Brown et al. (1977), there is a range of cumulative cyclic strains over which post-cyclic monotonic strength is improved without significant reduction in ductility (Figure 17), i.e. between 0.3% and 2% strain.

Crucially, these strengthened samples no longer liquefy. This supports the assertion that the Instability Line is a function of initial fabric which can be altered by load-induced fabric rearrangement. A proportion of the strength increase is related to greater dilatancy (i.e. the peak pore water pressure is reduced and beyond 3% strain, pore pressure dilation rates are higher) implying the fabric is rearranged into a less collapsible form. Beneficial fabric rearrangement is also implied by the post-cyclic strength and stiffness exceeding that of overconsolidated samples (c.f. Figure 12). Thus, another factor besides the change to stress state must be influencing the improved behaviour observed.

A minimum amount of fabric rearrangement in order to negate its precarious initial state is implied by a minimum cumulative strain for cyclic load treatment. The lowest-amplitude cyclic tests in Figure

17 do not accumulate plastic strain in excess of the liquefaction initiation strain (0.3%) and revert to intact, liquefiable behaviour during monotonic shear. As the minimum strain for stabilisation and the initiation strain for static and cyclic liquefaction correspond closely, it is implied that both phenomena require the same irreversible fabric rearrangement. Similarly, Wang et al. (2014) found the minimum strain for strengthening following cyclic load and consolidation corresponded closely with the cyclic yield strain; this large-strain yield threshold represents the point at which load-induced fabric changes dominate over the initial fabric in terms of behaviour. The dependence of treatment primarily upon cumulative cyclic strain (as opposed to cyclic stress) is further demonstrated by Cyclic 'C' series tests: liquefiable fabric is retained with ϵ_{pl} less than 0.3% regardless of the cyclic stress applied (Figure 18).

Conversely, if liquefaction is initiated before starting a monotonic shear stage, no stabilisation occurs and the sample continues to liquefy (test CC-154-7 in Figure 18, starting from $\epsilon_{pl} = 0.4\%$). The main difference between a liquefying and stable response appears to be the energy intensity used to reach the initiation strain, i.e. whether the strain is imposed as a single action or through multiple small actions. In the case of the former, a collapse mechanism is started and continues to propagate until 'recovery' strains (1.5%) are reached, whereas in the latter case internal stability is continually maintained.

4.4 Use of cyclic traffic loads as ground treatment

This observed strengthening of liquefiable soil through carefully applied cyclic preloading, i.e. below the liquefaction threshold stress but sufficiently large to gradually induce the necessary fabric rearrangement, is expected to have practical implications for improving foundation soils beneath temporary roads. Careful sequencing of heavy vehicle transits could thus greatly improve the haul road serviceability. By running smaller vehicles first, the risk of liquefaction or large plastic strains under subsequent larger loads is reduced. Most importantly, a vehicle which is sufficiently heavy to cause liquefaction (for a given road construction depth and soil profile) may be rendered safe by

carefully controlled passages of heavy haul vehicles of lesser weight. This approach should be coupled with an observational method which verifies this load-induced stabilisation. In this way, reduced road construction depths and therefore reduced costs (both in terms of raw materials and also logistics of bringing fill to site) can be attained.

Non-liquefying tests cross the Instability Line in effective stress space whilst remaining stable (i.e. below the liquefaction threshold stress), similarly to those overconsolidated by lowering cell pressure (Figure 19). Crossing the Instability Line, i.e. accumulation of a certain pore water pressure, and exceeding the initiation strain for liquefaction are closely linked. This phenomenon is important for monitoring purposes – monitoring strains in the order of 0.3% through settlement measurement is expected to be difficult and measurement errors are likely to obscure the actual strains, but pore water pressures corresponding to the Instability Line can be measured with greater reliability.

In order for the liquefiable soils to accumulate the necessary plastic strains during cyclic load treatment, it is important that the stress bulbs developed by the lighter vehicles cover a similar volume of soil (but not similar applied stresses) to those associated with the heaviest indivisible loads. Thus, it would be insufficient to simply use a lighter vehicle (for example a conventional lorry or large construction plant); instead a vehicle with the same wheel-base as the heaviest vehicle (although only transporting a proportion of the final load) is required to transit the haul road. These loads could be progressively increased until the desired treatment been achieved.

4.5. Sample disturbance

Initially, samples were consolidated to a length longer than required, and the top section trimmed using cheesewire; this was also intended to remove the drier and stiffer top section of the sample, improving uniformity. However water content distributions post-testing indicated no significant change and in some cases when the mould was removed a slight bulge at the sample top was apparent. Due to the potential for such disturbance on sensitive, liquefiable samples, the trimming

process was discontinued. This is clearly of importance when attempting to characterise a site using conventional ground investigation to obtain 'undisturbed' samples.

Some of these samples showing signs of disturbance were tested; there was a tendency to undergo greater volume change during consolidation (possibly resulting in the drier disturbed top section).

Under cyclic load, lower deformation increments, particularly during the first cycle of $\Delta q_{cyc}/\Delta q_{peak} = 1.92$ (i.e. cyclic liquefaction; Figure 20) is clear. It is thought this initial disturbance to the sensitive fabric allows a greater rearrangement into a denser, more stable form during subsequent consolidation. Santagata and Germaine (2005) also observed that carefully-controlled disturbance of liquefiable, normally consolidated samples followed by reconsolidation to the in situ stresses can reduce or remove their liquefaction potential and increase the ultimate strength. Without careful handling, soft liquefiable soil samples can be disturbed and develop stability unrepresentative of the in-situ deposit.

In this context, field sampling of soft, normally consolidated soils, with associated sampling-induced shear strains (Santagata and Germaine, 2005) and stress relief (Peters, 1988), carries a significant risk of underestimating the liquefaction potential due to disturbance. Santagata and Germaine (2005) found that reconsolidating to well above the in-situ stress and normalising results against consolidation stress after Ladd and Foott (1977) is effective for describing intact behaviour.

Reconstituting samples from bulk soil following the method outlined in Section 3 may also represent a cost-effective way to create representative samples. These samples will represent the worst-case in terms of liquefiability as ageing or chemical bonding during preparation is unlikely to take place to the same extent as in the field.

5. Observational design considerations

Using traffic sequencing to induce changes in the behaviour of liquefiable soils, by gradually incrementing vehicle weights as demonstrated through experimental tests herein, could present

attractive cost benefits for temporary haul road infrastructure. This method allows reduced construction depths on the basis that traffic loads can strengthen the subsoil over time; larger loads which are transited later are thus rendered safe. Bearing in mind the serious consequences associated with ground failure, this treatment through cyclic load must be verified; observational monitoring is thus necessary.

The first step in an observational design approach is to estimate a cyclic liquefaction threshold stress. Experimental results herein suggest this is close to the pre-liquefaction peak stress (q_{peak}); this simplification avoids the need for more complex testing, however this is currently only based on testing on a single soil and confirmation over a wider range of silts is necessary to provide confidence in such an approximation. A sequence of undrained cyclic tests (similar to the Cyclic 'B' tests) is recommended to estimate safe stress levels. From these tests, cyclic pore pressure and strain accumulation relationships can be estimated and used as a basis for interpreting in-situ monitoring data.

Monitoring of settlement at the surface, possibly supplemented by monitoring at depth (e.g. by down-borehole plate and rod settlement indicators) presents a simple and inexpensive method to determine when sufficient strain has been accumulated to stabilise the soil and thus when heavier vehicles are safe to pass. As strains may be relatively low (below 0.5%), piezometers monitoring in-situ pore water pressures, whilst potentially more expensive, may offer better insight on when treatment is effective. Cyclic loading levels for treatment will also need to exceed the volume change threshold. This can be determined from relatively straightforward undrained cyclic triaxial tests and corroborated via pore pressure monitoring.

The influence depth of the heaviest vehicles needs to be considered in the surcharging or cyclic pre-loading programme and associated monitoring; interaction between wheelsets can stress the ground to a much greater depth than usual (Krechowiecki-Shaw et al., 2017). Ideally a vehicle of the same (or larger) dimensions as those used to carry the largest load, but applying smaller stresses,

should be used in cyclic pre-loading. If surface settlement is monitored, a wide area, extending beyond the vehicle extents, should be covered so that strain at depth can be inferred. Finite element modelling of the anticipated load-strain-surface settlement response will be invaluable for verification and back-analysis.

Careful control and monitoring of a cyclic preload programme is necessary; liquefaction can propagate rapidly and once triggered, large permanent strains and a brittle response under subsequent loading can be expected. Using laboratory test data, plastic strain and pore water pressure accumulation rates for stresses above and below the threshold can be estimated. This can be compared to in-situ monitoring to indicate whether strain is accumulating too fast (i.e. indicating stresses above the actual threshold, at risk of triggering liquefaction) or too slow (i.e. that attempted improvement is not having the desired effect).

These experiments have not considered strengthening from consolidation of residual excess pore pressures following cyclic pre-loading. Wang et al. (2014, 2015) indicate it may be significant, particularly following liquefaction; i.e. up to three times the intact strength for accumulation of 8.5% strain (Wang et al., 2014). However undrained loading following such large strains is brittle and prone to shear banding. The risk of shear banding may be reduced by reconsolidation, which reduces dilatancy (Wang et al., 2015, 2016), but reconsolidated tests are still more brittle than intact tests (Wang et al.; 2014, 2015). A better understanding of the effects of reconsolidation on shear banding risk is required if cyclic loading and consolidation are used to develop significantly increased strength through inducing large strains.

6. Conclusions

Metastable liquefaction of soil, characterised by a loss of strength and rapid strain accumulation, is initiated with little advanced warning following a small initial disturbance (in the order of 0.1% strain), but can only occur if specific initial conditions are met, i.e. a contractant soil and precarious

initial fabric which has a sufficiently high potential energy state to trigger a chain reaction. Cyclic stresses exceeding the liquefaction threshold stress (a function of the initial fabric) must be applied and coincide with the cumulative strain exceeding the liquefaction initiation strain, in order to trigger liquefaction. At this point, the effective stress path crosses the Instability Line in q, p' space (also a function of the initial fabric). Liquefaction is predominantly observed in loose sands and normally consolidated, low plasticity silts and clays.

This paper demonstrates liquefaction can be averted either by statically overconsolidating the soil (which may be too expensive and time-consuming as a treatment for temporary roads), or applying a sequence of medium-strain cyclic loads to gradually stabilise the liquefiable fabric and induce the effects of overconsolidation (i.e. unload-reload history and reduced contraction in shear).

Liquefaction is averted by gradually accumulating plastic strain until it exceeds the liquefaction (large-strain) threshold: this can also be described by the stress state crossing the Instability Line in stable (sub-threshold stress or drained) conditions. It is expected that plastic strain energy input is an important factor; repetition of small loads may be sufficient to gradually mobilise small numbers of particles and rearrange the fabric without precipitating a collapse that would occur if the same strain was applied in a smaller number of cycles. Effective treatment requires cyclic load application which exceeds the volume change (medium-strain) threshold but is below the liquefaction threshold stress.

Careful pre-loading with lighter loads may be an effective method for treating liquefiable soil beneath temporary roads carrying large indivisible loads. To be effective, pre-load vehicles need to be of similar dimensions to the main loads to treat similarly sized stress bulbs. Treatment should be carefully monitored to determine when improvement is effective; piezometers at depth and settlement monitoring will be useful in this respect and will also assist in back-analysing predictive models.

The silt soil tested herein failed in a brittle manner by initiation of a shear band, governed by the total strain developed in undrained shear (monotonic, cyclic or combined). Whilst temporary roads may be able to deal with a certain amount of strain by re-grading, it seems sensible to maintain cumulative strains well below that expected to cause shear banding.

Disturbance during sample preparation can induce an apparent overconsolidation and was found to reduce the liquefaction potential. Laboratory tests on apparently undisturbed samples recovered from site may underestimate the risk of liquefaction. Reconsolidation following Ladd and Foott (1977) may be necessary to recreate realistic in-situ behaviour in laboratory tests. Alternatively, the slurry consolidation method detailed herein may be viable for cost-efficient investigation of liquefaction risk.

This paper has only considered cyclic loading without drainage of excess pore pressures; strength gains from consolidation after cyclic loading (observed by others) can be significant. Cyclic pre-loading, allowing consolidation, could thus be a very effective method for strengthening weak subsoils generally but may require sizeable strains to be developed incrementally. Further research into this phenomenon, particularly the interaction with shear band failure, is recommended.

References

- Andersen, K. H. 2009. Bearing capacity under cyclic loading - offshore, along the coast and on land. The 21st Bjerrum Lecture presented in Oslo, 23 November 2007. Canadian Geotechnical Journal, 46(5): 513-535, 10.1139/T09-003.
- Andrews, D. C. A., Martin, G. R. 2000. Criteria for Liquefaction of Silty Soils. Proceedings of 12th World Conference on Earthquake Engineering, Auckland, New Zealand, 30th January - 4th February 2000.
- Atkinson, J. H. 2000. Non-linear soil stiffness in routine design. Geotechnique 50(5), 487-508.

621 Been, K., Jefferies, M.G. 1985. A state parameter for sand. *Geotechnique* 35(2), 99-122.

622 Bishop, A.W., Green, G.E. 1965. The influence of end restraint on the compression

623 strength of a cohesionless soil. *Géotechnique*, 15(3): 243-266.

624 Bradshaw, A. S., Baxter, C. D. P. 2007. Sample Preparation of Silts for Liquefaction testing.

625 *Geotechnical Testing Journal* 30(4), Paper ID GTJ00206.

626 BSI (British Standards Institution). 1990. BS 1377-2:1990 - Methods of test for soils for civil

627 engineering purposes — Part 2: Classification tests

628 BSI (British Standards Institution). 2015. BS 5930:2015 - Code of practice for ground investigations.

629 Brown, S. F., Andersen, K. H., McElvaney, J. 1977. The Effect of Drainage on Cyclic Loading of Clay.

630 *Proceedings, 9th International Conference of Soil Mechanics and Foundation Engineering*. 2: 195-

631 200. Tokyo.

632 D'Appolonia, D. J., Poulos H. G., and Ladd C. C. (1971). *Initial Settlement of Structures on Clay*. ASCE

633 *Journal of the Soil Mechanics and Foundations Division* 97(10): 1359-1377.

634 Dean, E. T. R. 2015. Particle mechanics approach to continuum constitutive modelling. *Geotechnical*

635 *Research* 2(1), 3-34.

636 Díaz-Rodríguez, J. A., López-Molina, J. A. 2008. Strain thresholds in soil dynamics. 14th World

637 *Conference on Earthquake Engineering*. October 12-17th 2008, Beijing, China. .

638 Díaz-Rodríguez, J. A., Santamarina, J. C. 2001. Mexico city soil behavior at different strains:

639 *Observations and physical interpretation*. *Journal of Geotechnical and Geoenvironmental*

640 *Engineering* 127 (9).

641 Doanh, T., Finge, Z., and Boucq, S. 2012. Effects of Previous Deviatoric Strain Histories on the
 642 Undrained Behaviour of Hostun RF Loose Sand. *ASCE Journal of Geotechnical and Geological*
 643 *Engineering* 30: 697-712.

644 Edwards, S. F., Brujić, J., Makse, H. A. 2004. A basis for the statistical mechanics of granular systems.
 645 *Unifying concepts in Granular Media and Glasses*. Elsevier, Amsterdam.

646 Erken, A., Ulker, B. M. C. 2007. Effect of cyclic loading on monotonic shear strength of fine-grained
 647 soils. *Engineering Geology* 89: 243–257.

648 Frost, M.W, Fleming, P.R, Rogers, C. D. F. 2004. Cyclic triaxial tests on clay subgrades for analytical
 649 pavement design. *ASCE Journal of Transportation Engineering* 130(3), 378-386.

650 Gong, G. 2008. DEM Simulations of Drained and Undrained Behaviour (PhD thesis). University of
 651 Birmingham Department of Civil Engineering.

652 Gu, X., Huang, M. Qian, J. 2014. DEM investigation on the evolution of microstructure in granular
 653 soils under shearing. *Granular Matter* 16, 91-106.

654 Head, K. H. 1986. *Manual of Soil Laboratory Testing Volume 3: Effective Stress Tests*. ELE
 655 International Ltd. . Pentech Press, London.

656 Heath, D. L., Shenton, M. J., Sparrow, R. W., Waters, J. M. 1972. Design of Conventional Rail Track
 657 Foundations. *ICE Proceedings*, 51(2), 251-267.

658 Hsu, C., Vucetic, M. 2006. Threshold shear strain for cyclic pore water pressure in cohesive soils.
 659 *ASCE Journal of Geotechnical and Geoenvironmental Engineering* 132: 1325-1335.

660 Hu, M., O'Sullivan, C., Jardine, R.R., Jiang, M. 2010. Stress-induced anisotropy in sand under cyclic
 661 loading. *Granular Matter* 12, 369-476. Springer-Verlag.

662 Kirkpatrick, W. M., Belshaw, D. J. 1968. On the Interpretation of the Triaxial Test. *Geotechnique* 18:
663 336-350.

664 Krechowiecki-Shaw, C. J., Royal, A.C., Jefferson, I., Ghataora, G. S. 2017. Routes for exceptional loads:
665 a new soil mechanics perspective. *Proceedings of the ICE: Transport* In Press.

666 Kruyt, N. P. 2010. Micromechanical study of plasticity of granular materials. *Comptes Rendus*
667 *Mecanique* 338, 596-603. Elsevier.

668 Ladd , C.C., Foott, R. 1977. New design procedure for stability of soft clays. *Journal of the*
669 *Geotechnical Engineering Division of the ASCE* 100 (GT4): 763–779

670 Lade, P. V. 1994. Instability and Liquefaction of Granular Materials. *Computers and Geotechnics* 16,
671 123-151. Elsevier.

672 Lee, K. L. 1978. End restraint effects on undrained static triaxial strength of sand. *Journal of the*
673 *Geotechnical Engineering Division of the ASCE* 104(GT6):687–704

674 Lee, K. L., Vernese, F. J. 1978. End restraint effects on cyclic triaxial strength of sand. *Journal of the*
675 *Geotechnical Engineering Division of the ASCE* 104(GT6): 705–719

676 Li, L., Dan, H., Wang, L. 2011. Undrained behavior of natural marine clay under cyclic loading. *Ocean*
677 *Engineering* 38, 1792-1805. Elsevier.

678 Lin, H., Penumadu, D. 2005. Experimental Investigation on Principal Stress Rotation in Kaolin Clay.
679 *ASCE Journal of Geotechnical and Geoenvironmental Engineering* 131(5), 633-642.

680 Lunne, T., Berre T., Andersen, K. H., Strandvik S., Sjursen, M. (2006). Effects of sample disturbance
681 and consolidation procedures on measured shear strength of soft marine Norwegian clays. *Canadian*
682 *Geotechnical Journal* 43: 726-750.

683 Madabhushi, S.S.C., Haigh, S.K. (2015). Investigating the changing deformation mechanism beneath
684 shallow foundations. *Géotechnique* 65(8): 684–693

685 Muhunthan, B., Worthen, D. L. 2011. Critical state framework for liquefaction of fine grained soils.
686 *Engineering Geology* 117, 2-11. Elsevier.

687 Nova, R. 2010. Controllability of Geotechnical Tests and their Relationship to the Instability of Soils.
688 *Micromechanics of Failure in Granular Geomaterials*, Ed. F. Nicot & R. Wan, 1-34. ISTE and John
689 Wiley & Sons.

690 O'Reilly, M.P., Brown, S.F., Austin, G. 1988. Some Observations on the Creep Behaviour of a Silty
691 Clay. *International Conference on Rheology and Soil Mechanics*, Coventry. Ed. M. J. Keedwell, p44-
692 58. Elsevier Applied Science.

693 Osman, A. S., Boulton, M. D. (2005). Simple plasticity-based prediction of the undrained settlement
694 of shallow circular foundations on clay. *Geotechnique* 55(6), 435-447.

695 Overy, R. F. 1982. The Behaviour of Anisotropically Consolidated Silty Clay Under Cyclic Loading (PhD
696 Thesis). University of Nottingham Department of Civil Engineering.

697 Peters, J. F. 1988. Determination of undrained shear strength of low plasticity clays. *Advanced*
698 *Triaxial Testing of Soil and Rock*, ASTM STP 977, 460-474. American Society for Testing and Materials.

699 Sadrekarimi, A. 2014. Static liquefaction-triggering analysis considering soil dilatancy. *Soils and*
700 *Foundations* 54: 955–966

701 Santagata, M., Germaine, J. T. 2005. Effect of OCR on sampling disturbance of cohesive soils and
702 evaluation of laboratory reconsolidation procedures. *Canadian Geotechnical Journal* 42: 459-474.
703 NRC Canada.

704 Schofield, A., Wroth, P. 1968. *Critical State Soil Mechanics*. McGraw Hill. London.

705 Sheng, D., Westerburg, B., Mattsson, H., Axelsson, K. 1997. Effects of End Restraint and Strain Rate in
706 Triaxial Tests. *Computers and Geotechnics* 21(3): 163-182.

707 Sitharam, T. G., Vinod, J. S. 2009. Critical state behaviour of granular materials from isotropic and
708 rebounded paths: DEM simulations. *Granular Matter* 11:33–42

709 Togrol, E., Güler, E. 1984. Effect of repeated loading on the strength of clay. *Soil Dynamics and*
710 *Earthquake Engineering* 3(4), 184-190. CML Publications.

711 Valls-Marquez, M., Chapman, D. N., Ghataora, G. S. 2008. Preparation of K0-consolidated
712 reconstituted samples in the laboratory. *International Journal of Geotechnical Engineering* 2: 343-
713 354.

714 Wang, S., Luna, R. 2012. Monotonic behavior of Mississippi River Valley Silt in Triaxial Compression.
715 *Journal of Geotechnical and Geoenvironmental Engineering* 138 (4): 516–525.

716 Wang, S., Luna, R., Onyejekwe, S. 2015. Postliquefaction behavior of low-plasticity silt at various
717 degrees of reconsolidation. *Soil Dynamics and Earthquake Engineering* 75, 259-264.

718 Wang, S., Luna, R., Onyejekwe, S. 2016. Effect of Initial Consolidation Condition on Post-Liquefaction
719 Undrained Monotonic Shear Behavior of Mississippi River Valley Silt. *Journal of Geotechnical and*
720 *Geoenvironmental Engineering* 142(2): 04015075-1 to 11.

721

722 Wang, S., Luna, R., Stephenson, R. W. 2011. A slurry consolidation approach to reconstitute low-
723 plasticity silt specimens for laboratory triaxial testing. *Geotechnical Testing Journal* 34(4), Paper ID
724 GTJ103529.

725

Wang, S., Onyejekwe, S., Yang, J. 2014. Threshold Strain for Postcyclic Shear Strength Change of Mississippi River Valley Silt Due to Cyclic Triaxial Loading. *Journal of Testing and Evaluation* 42(1): 1-9.

Ward, S. J. 1983. The stability of a silty clay under repeated loading (PhD thesis). Loughborough University.

Yamamuro, J. A., Lade, P. V. 1999. Experiments and modelling of silty sands susceptible to static liquefaction. *Mechanics of Cohesive-Frictional Materials* 4, 545-564. John Wiley & Sons Ltd.

Zhang, H., Garga, V. K. 1997. Quasi-steady state: a real behaviour? *Canadian Geotechnical Journal* 34: 749–761

Zhao, J. & Guo, N. 2015. The interplay between anisotropy and strain localisation in granular soils: a multiscale insight. *Géotechnique* 65(8), 642–656.

List of tables

Table 1: Summary of intact monotonic tests

Test	Consolidation σ'_3 (kPa)	Consolidation σ'_1 (kPa)	Liquefaction stress increment Δq_{peak} (kPa)	Ultimate strength Δq_{ult} (kPa)	Final void ratio, e	Δe_c
M-01	150	337	26	68	0.490	0.073
M-02	150	337	29	81	0.489	0.070
M-03	150	348	24	50	0.490	0.062
M-04	150	316	28	42	0.492	0.057
ML-05	150	336	26	69	0.486	0.059
M-06	75	168	11	11	0.492	0.029
M-07	50	112	7	16	0.493	0.025
M-08	200	445	38	N/A	0.460	0.111

Table 2: Summary of overconsolidated monotonic tests

Test	Consolidation σ'_3 max/final (kPa)	Consolidation σ'_1 max/final (kPa)	Δq_{ult} (kPa)	Final void ratio, e	Δe_c max/final
M-09	150/100	335/267	68	0.490	0.077/0.001
M-10	150/119	337/310	81	0.489	0.064/0.0003

Table 3: Summary of cyclic series A tests (no correction for increasing area, see Figure 5). N.b. all tests are consolidated to $\sigma'_1 = 150\text{kPa}$, $K = 0.45$.

Test	Δq_{cyc} (kPa)	$\Delta q_{cyc}/$ Δq_{peak} (kPa)	N	Final void ratio, e	Δe_c	Final ε_{pl} (%)	Notes
CA-96	25	0.96	200	0.482	0.061	1.7	Post-cyclic sheared
CA-154-1	40	1.54	200	0.489	0.064	5.0	Post-cyclic sheared
CA-154-2	40	1.54	200	0.474	0.063	8.0	Post-cyclic sheared
CA-154-3	40	1.54	200	0.490	0.068	7.3	
CA-154-4	40	1.54	200	0.482	0.051	7.4	Post-cyclic sheared
CAL-154-5	40	1.54	200	0.481	0.070	5.9	Post-cyclic sheared
CA-154-6	40	1.54	169	0.456	0.074	1.4	Deviator stress lost (control error) – unloaded and reloaded
CA-192-1	50	1.92	129	0.484	0.070	16.3	Shear banding during cyclic
CA-192-2d	50	1.92	135	0.476	0.076	4.6	
CA-192-3d	50	1.92	200	0.468	0.133	4.2	
CAL-192-4	50	1.92	200	0.476	0.067	11.8	
CA-192-5d	50	1.92	200	0.459	0.077	6.1	
CA-192-6	50	1.92	19	0.481	0.067	10.3	Shear banding during cyclic

Table 4: Summary of cyclic series B tests (corrected for increasing area, see Figure 5). N.b. all tests are consolidated to $\sigma'_1 = 150\text{kPa}$, $K = 0.45$.

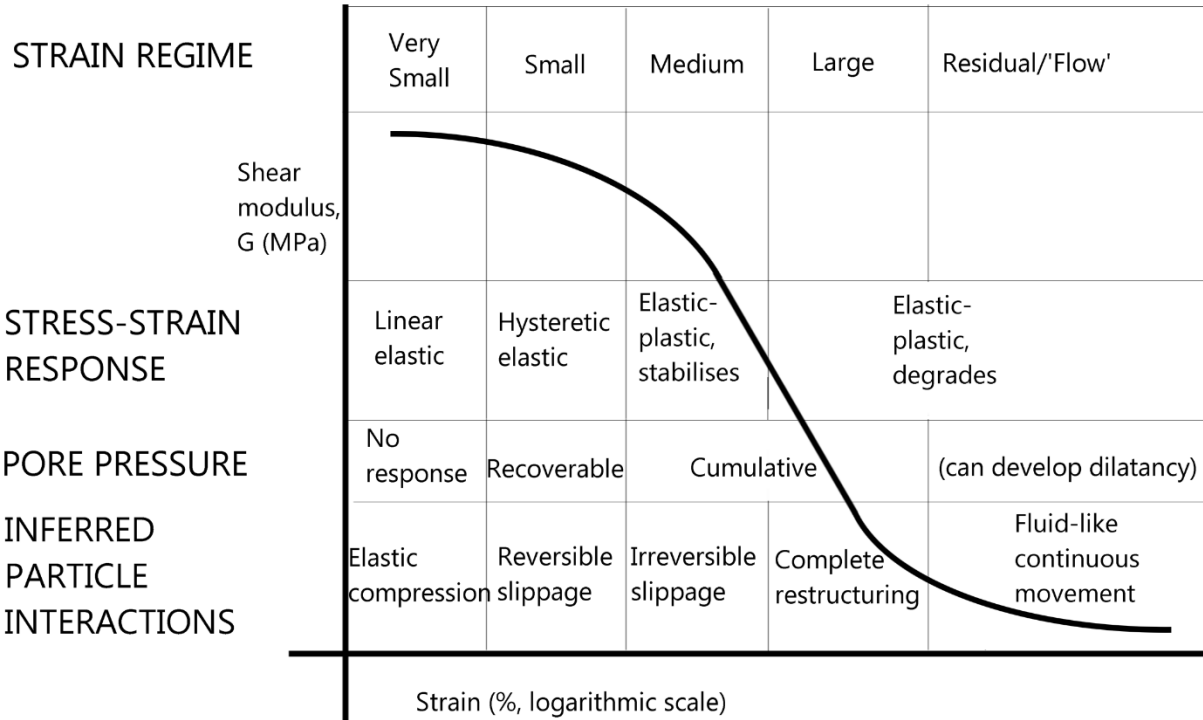
Test	Δq_{cyc} (kPa)	$\Delta q_{cyc}/$ Δq_{peak} (kPa)	N	Final void ratio, e	Δe_c	Final ε_{pl} (%)	Notes
CB-31-1	8	0.31	200	0.479	0.066	0.06	Post-cyclic sheared
CB-31-2	8	0.31	200	0.483	0.063	0.05	
CB-31/77	8/20	0.31/0.77	50/200	0.467	0.077	0.01/0.5	Post-cyclic sheared
CB-57	15	0.57	200	0.473	0.060	0.3	Post-cyclic sheared
CB-57/77	15	0.57	670/500	0.474	0.075	0.1/1.0	0.1Hz cyclic frequency, Post-cyclic sheared
CB-77-1	20	0.77	200	0.460	0.057	0.7	Post-cyclic sheared
CB-77-2	20	0.77	500	0.474	0.108	1.1	0.1Hz cyclic frequency
CB-96-1	25	0.96	200	0.482	0.053	8.7	Post-cyclic sheared
CB-96-2	25	0.96	840	0.478	0.068	7.4	0.1Hz cyclic frequency
CB-154		0.154	100	0.466	0.044	9.4	
CB-173	45	0.173	200	0.473	0.050	15.5	

Table 5: Summary of cyclic series C tests (corrected for increasing area, see Figure 5). N.b. all tests are consolidated to $\sigma'_1 = 150\text{kPa}$, $K = 0.45$.

Test	Δq_{cyc} (kPa)	$\Delta q_{cyc}/\Delta q_{peak}$ (kPa)	N	Final void ratio, e	Δe_c	Final ϵ_{pl} (%)	Notes
CC-154-1	40	1.54	1	0.480	0.064	0.2	Post-cyclic sheared
CC-154-7	40	1.54	7	0.468	0.073	0.4	0.1Hz cyclic frequency, post-cyclic sheared
CC-77-10	20	0.77	10	0.479	0.072	0.1	Post-cyclic sheared

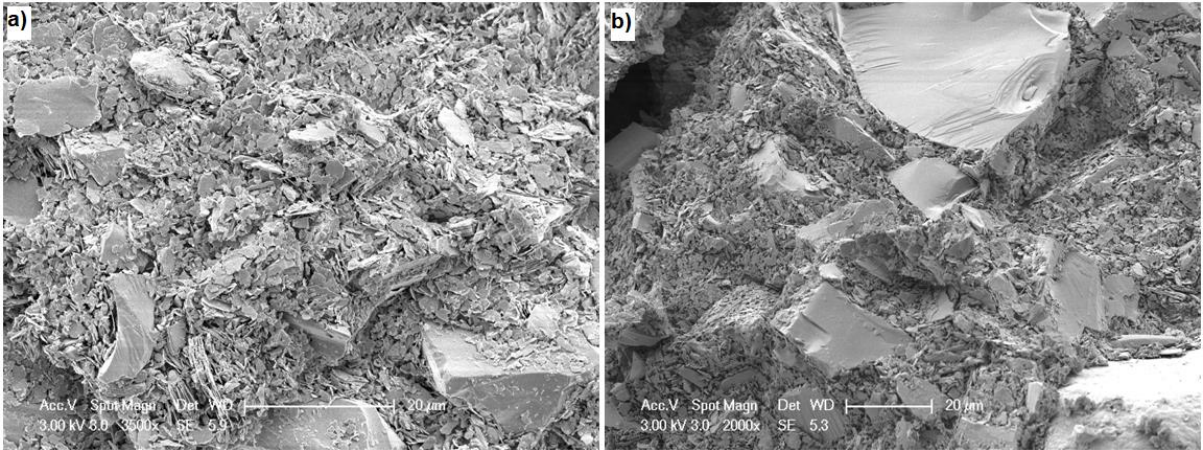
749

750 **List of figures**



751

752 Figure 1: Strain regimes after Díaz-Rodríguez and López-Molina (2008) with possible particle
753 interactions inferred from DEM literature



754

Figure 2: Electron micrograph of vertically-oriented slices from samples of the Silt Mix used in tests. a) – prepared by compaction, random particle arrangements. b) - prepared by slurry consolidation, preferential orientation.

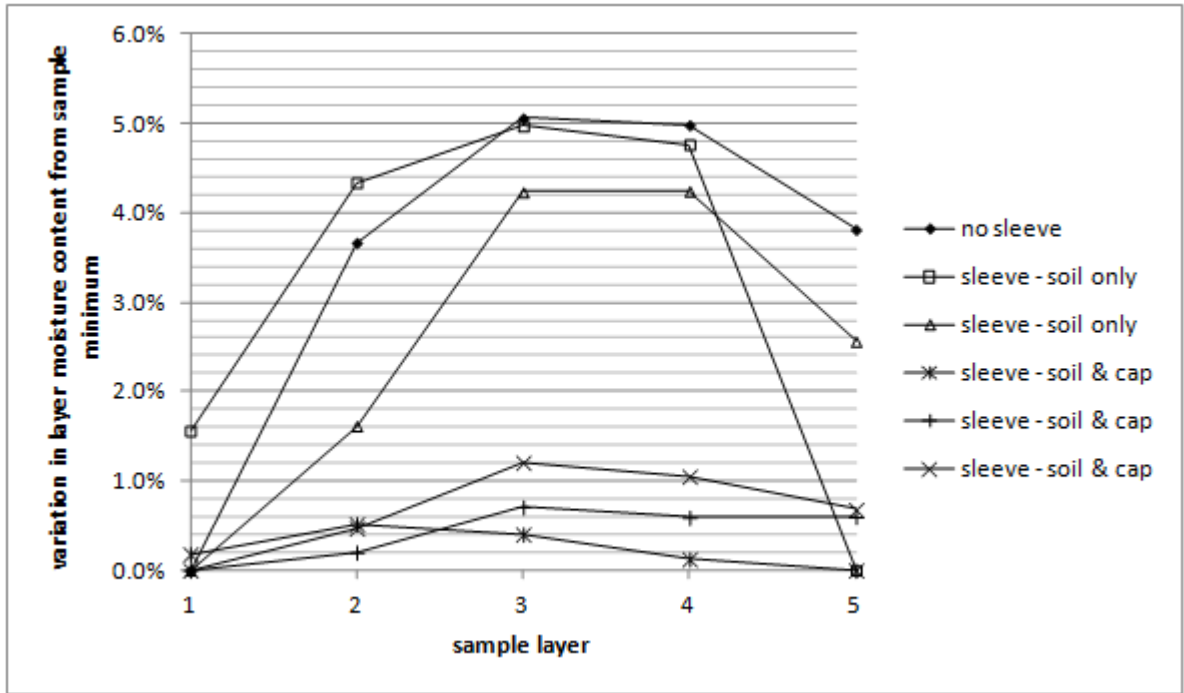


Figure 3: Intra-sample water content variation from top (layer 1) to bottom (layer 5) of 6 separate test samples with different mould arrangements; with and without a 'sleeve' comprising a 100mm diameter triaxial membrane, either fixed to the mould (soil only) or extended over the top cap (soil & cap).

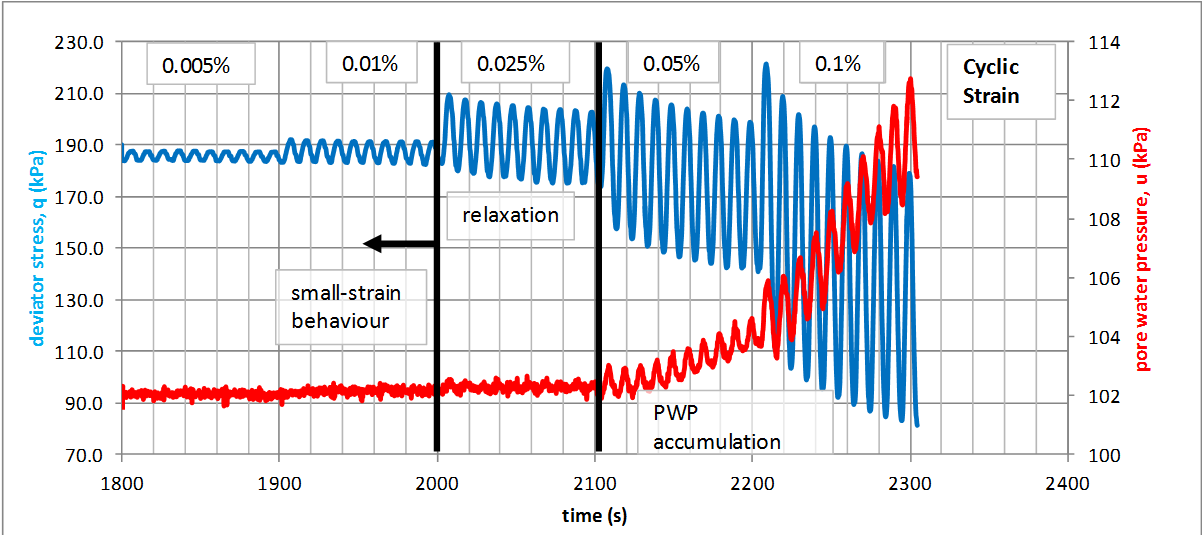


Figure 4: Strain-controlled testing to determine the initiation of medium-strain plastic behaviour by detection of soil skeleton contraction (rising pore water pressure) and plastic strain (relaxation of the deviator stress). Note differences in strain between these different behaviours, expected to be as a result of base pore pressure measurement and stress/strain non-uniformities from end restraint.

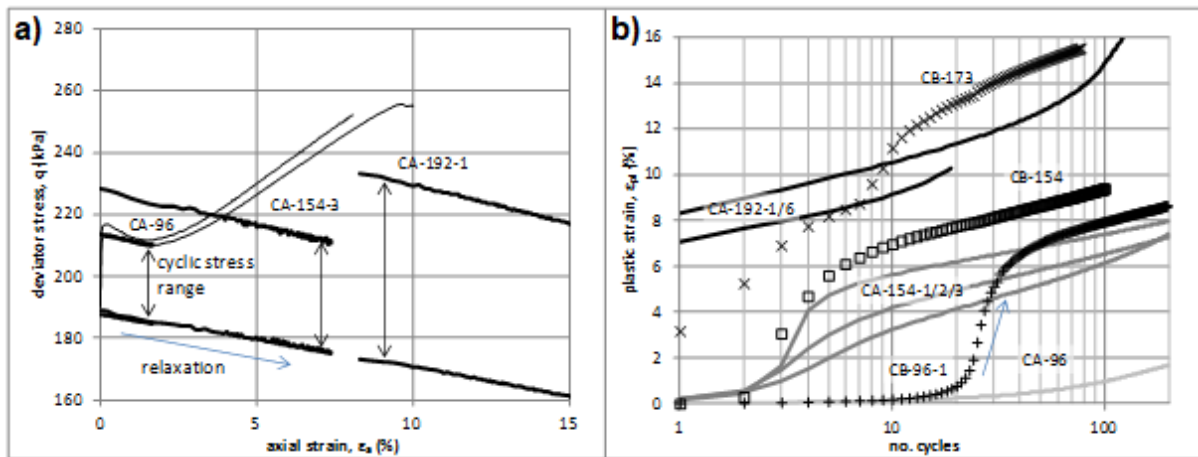


Figure 5: a) Maximum cyclic deviator stress (q_{max}) for cyclic 'A' series tests, i.e. without manual corrections applied (thick lines). Monotonic tests M-02 and M-03 (thin lines) shown for comparison; note that even the relaxation of ~ 4 kPa from $q_{max} = 214$ kPa to 210 kPa is significant in this context. b) increased strain accumulation and lower threshold stress due to manual stress correction (i.e. CA-96-1 is stable but relaxation corrected test CB-96 liquefies) as a result of increased axial force (according to Equation 1).

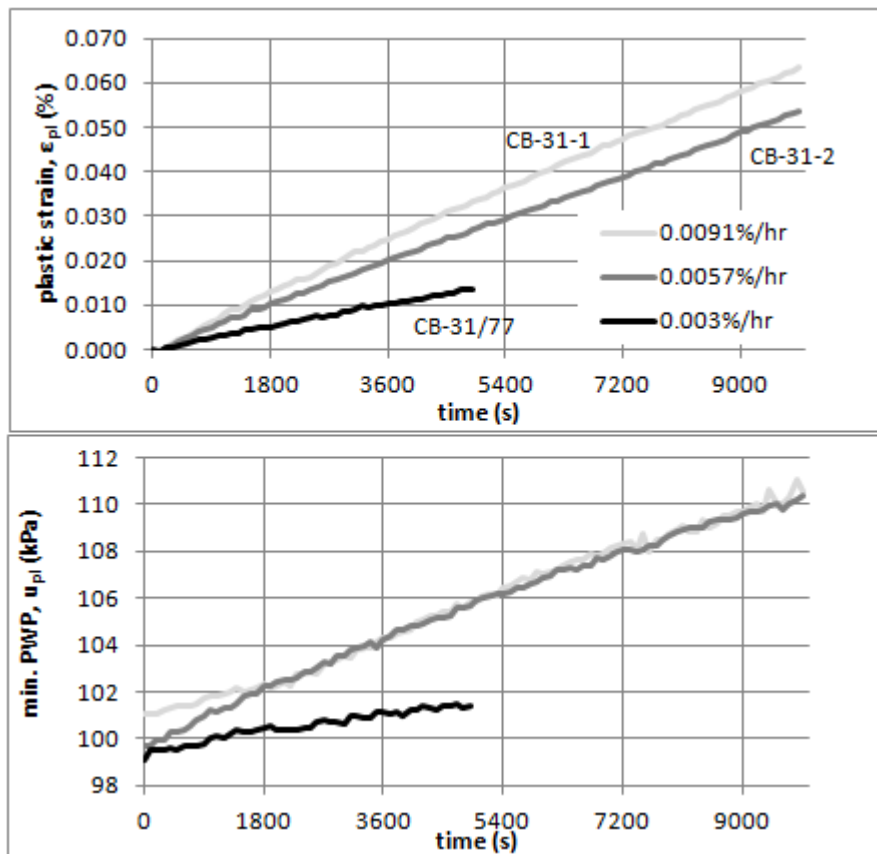


Figure 6: Plastic strain accumulation rates for low-amplitude, small-strain ($\Delta q_{cyc} = 8$ kPa) cyclic tests experiencing different creep strain rates (in legend) at the end of consolidation, achieved by longer secondary consolidation periods.

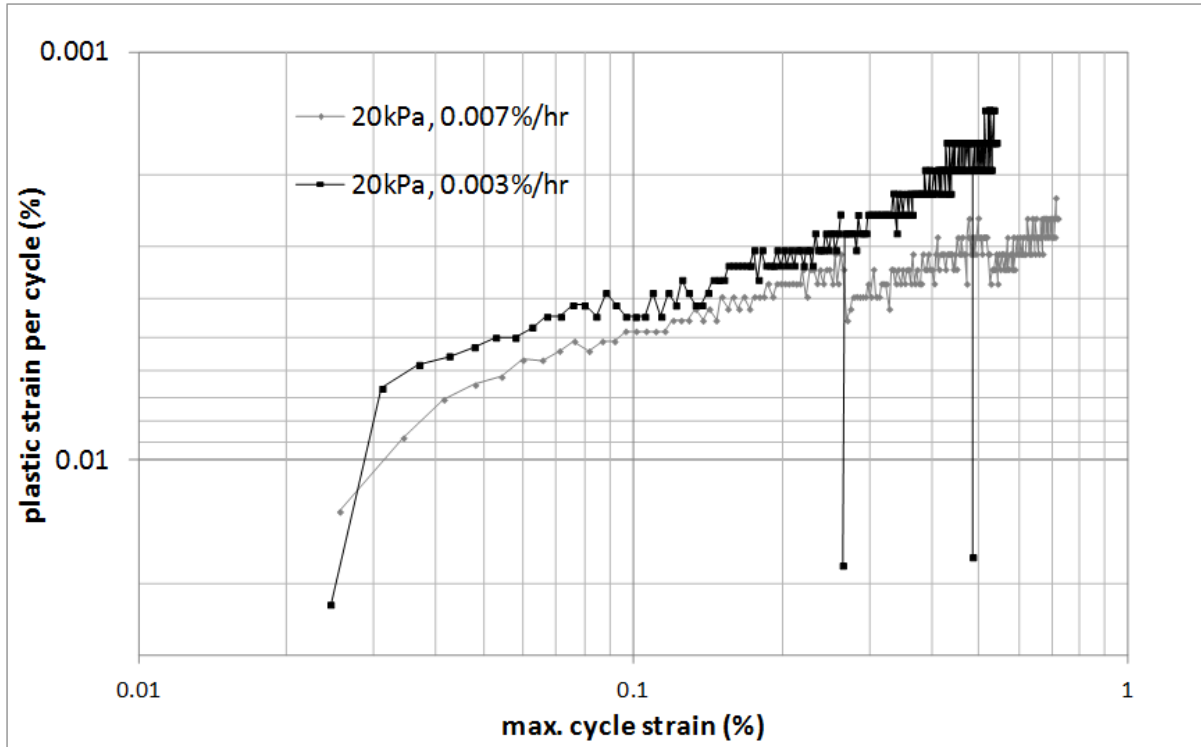


Figure 7: Comparison of medium-strain, stabilising ($\Delta q_{cyc} = 20\text{kPa}$) cyclic tests with differing final consolidation creep rates. Strains per cycle equivalent to 30x final consolidation creep rates are 0.006% and 0.0024% respectively.

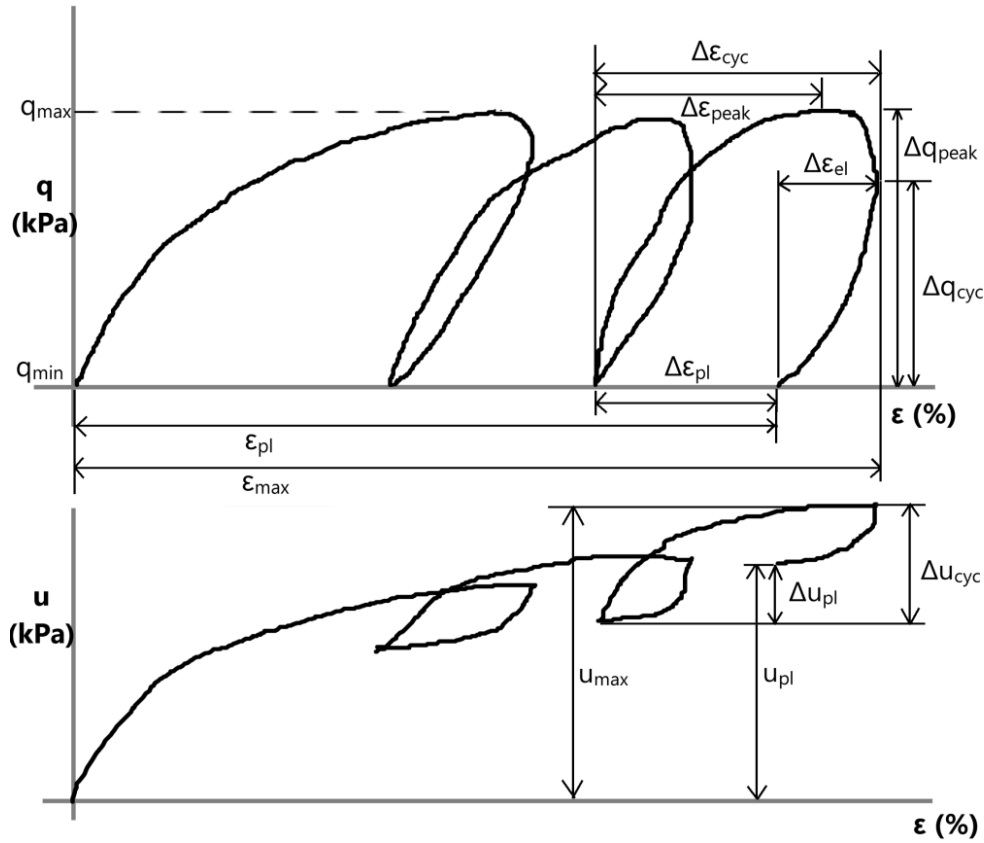


Figure 8: Definition of cyclic stress and strain symbols

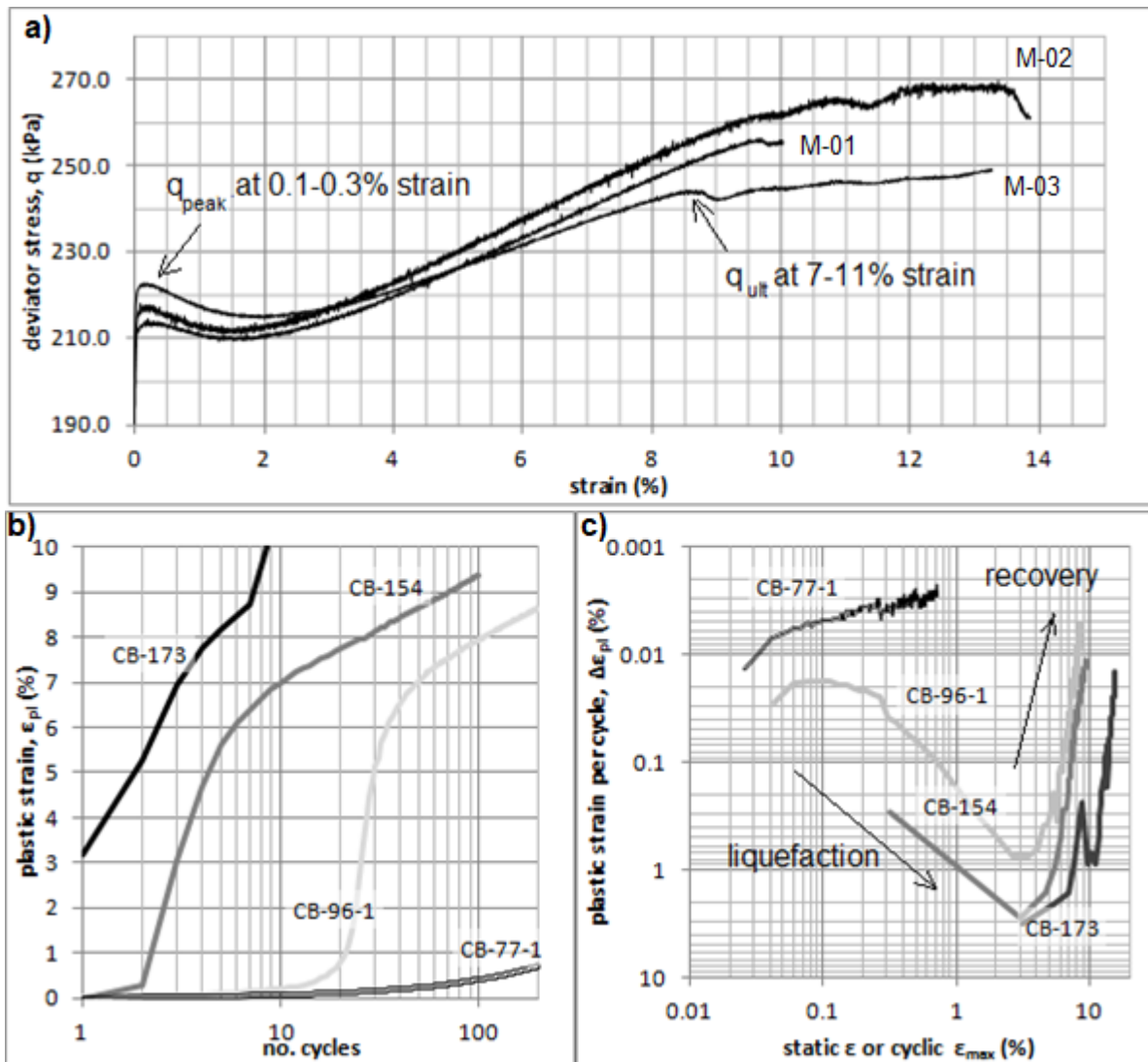


Figure 9: Static liquefaction and cyclic threshold stress effect for Silt Mix soil samples. a) Stress-strain relationship for monotonic loading. b) Accumulation of strain under varying cyclic stresses (area-corrected tests). c) Accumulation of plastic strain as a function of maximum strain achieved in the corresponding cycle; note similarity in strain levels to initiation of static liquefaction and recovery above.

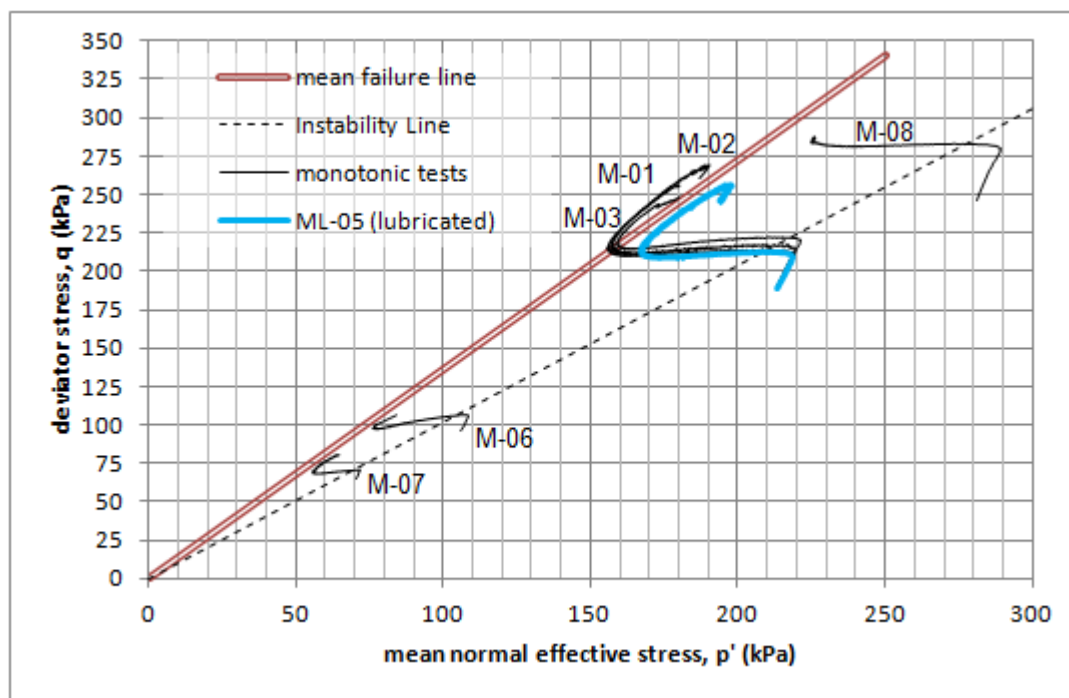


Figure 10: Undrained effective stress paths of monotonic tests indicating stress states for instability and failure

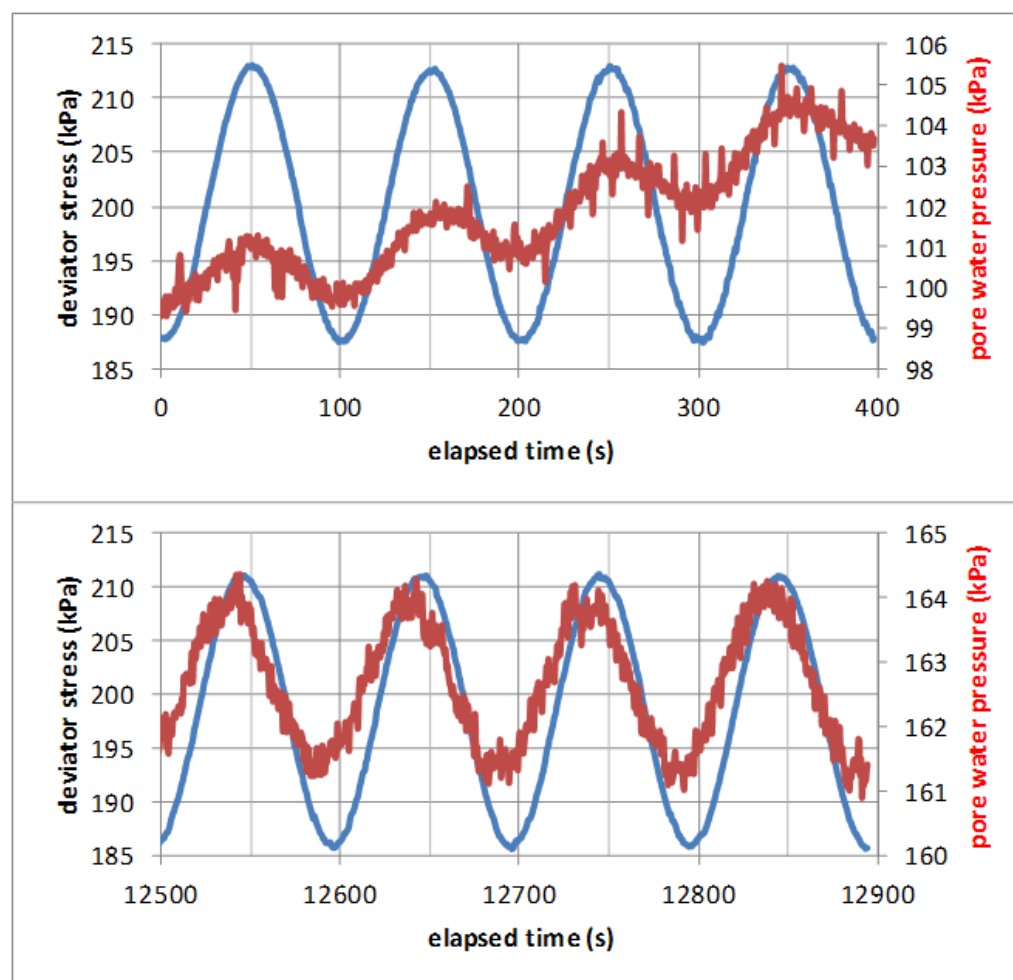


Figure 11: Pore water pressure response compared to stress pulse for test CB-96-1. Above: at small strains (0 to 0.1%); contractant response to shear, PWP lagging the stress pulse. Below: at large strains (8.1 to 8.2%); possible dilation at maximum shear, PWP slightly leading the stress pulse.

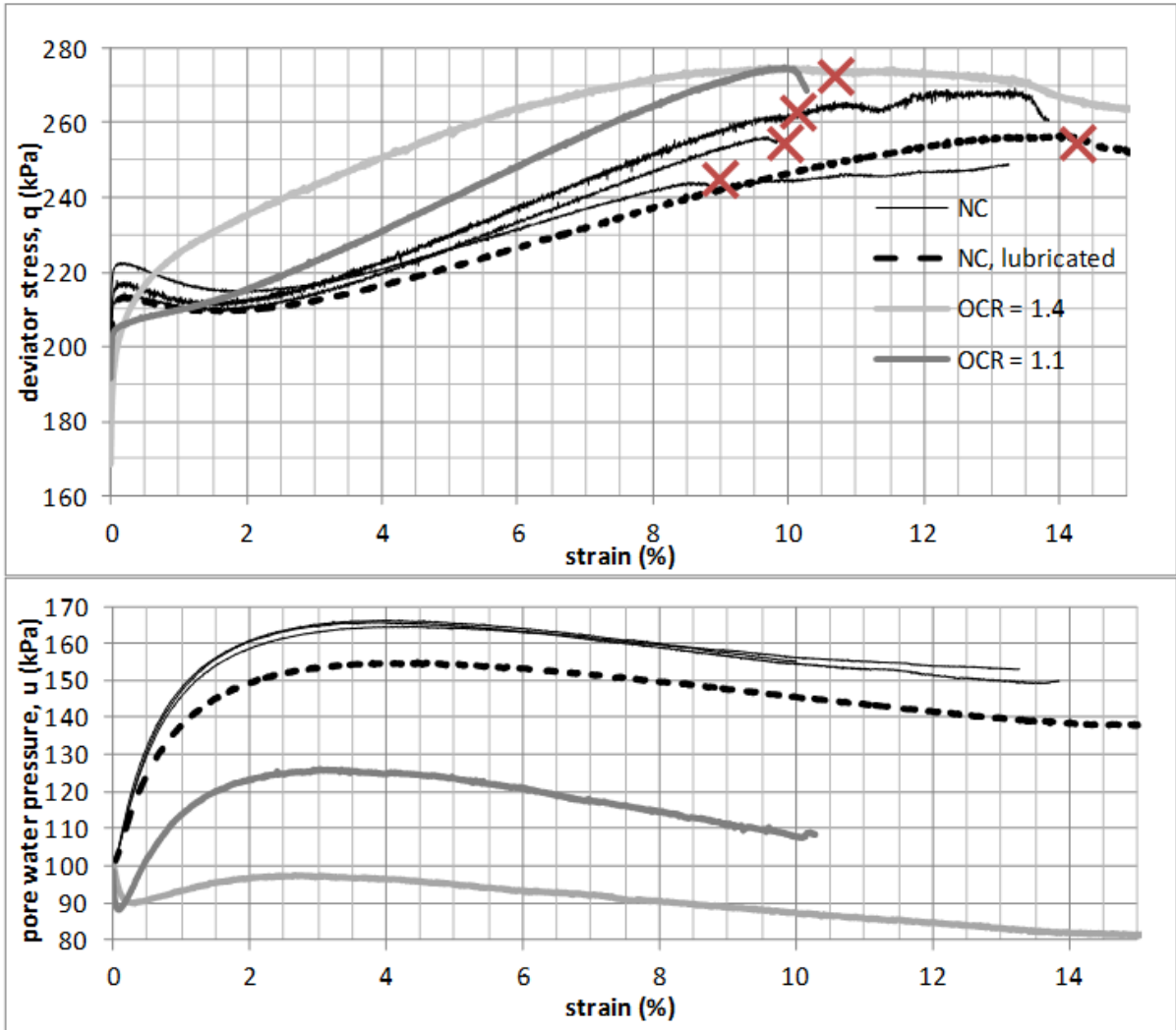


Figure 12: Changes to undrained shear response and prevention of liquefaction from increasing overconsolidation. 'X' marks indicate initiation of shear bands. Also note increased failure strain of lubricated-end sample (ML-05).

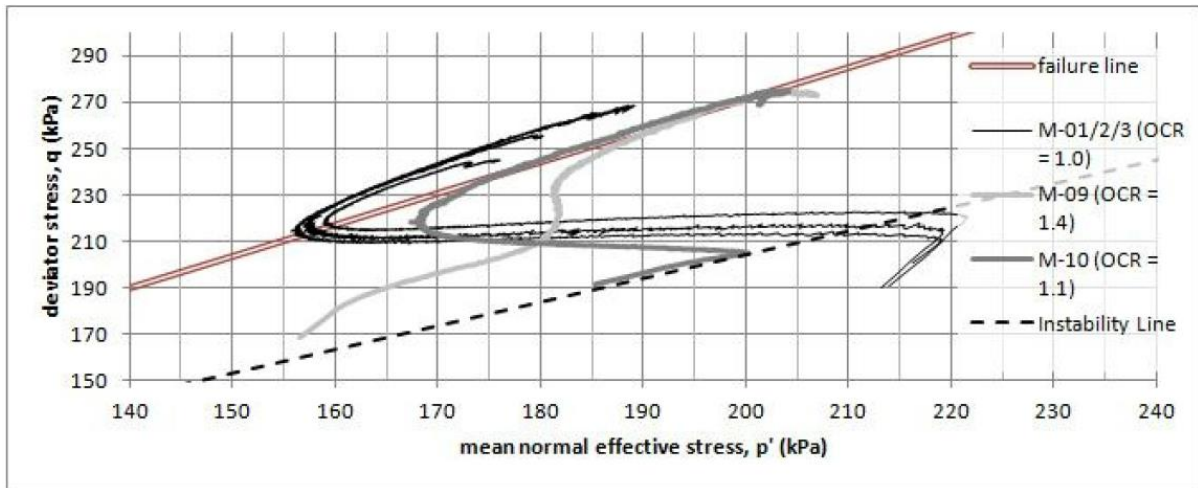


Figure 13: Undrained effective stress paths of normally consolidated and overconsolidated monotonic tests with reference to the Instability Line, which separates intact (liquefiable) and stabilised responses

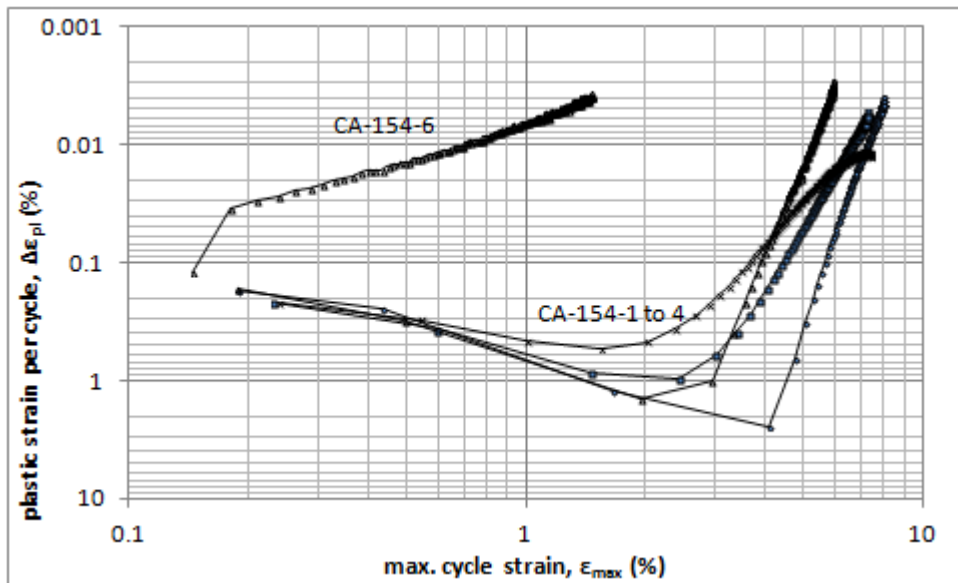
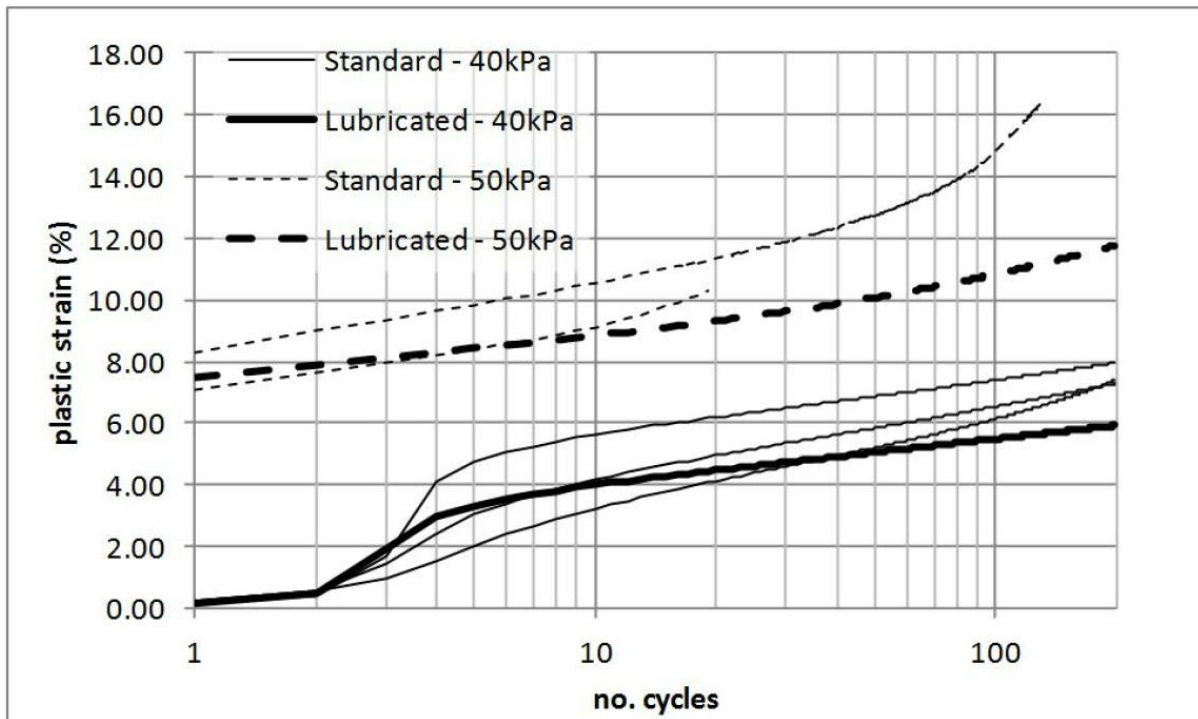


Figure 14: Reduction in plastic strain accumulation resulting from complete removal and re-application of maximum deviator stress (CA-154-6) during normal consolidation (c.f. CA-154-1 to 4, for which consolidation stress was not interrupted)



811

812 Figure 15: Reduction in strain accumulation rates within very large-strain regime resulting from end
813 lubrication for Series 'A' tests (i.e. without stress-correction), in agreement with findings of Lee and
814 Vernese (1978).

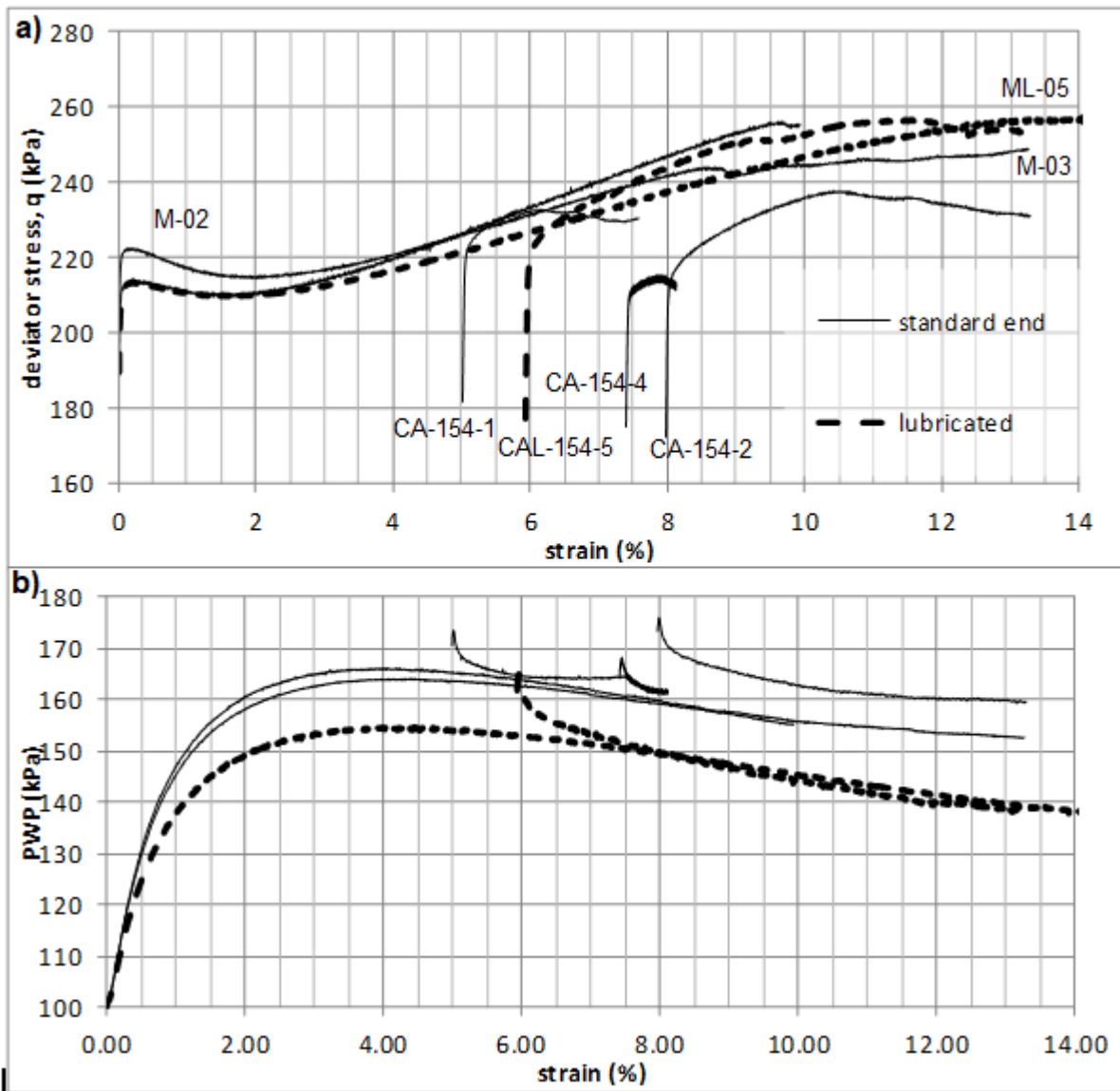
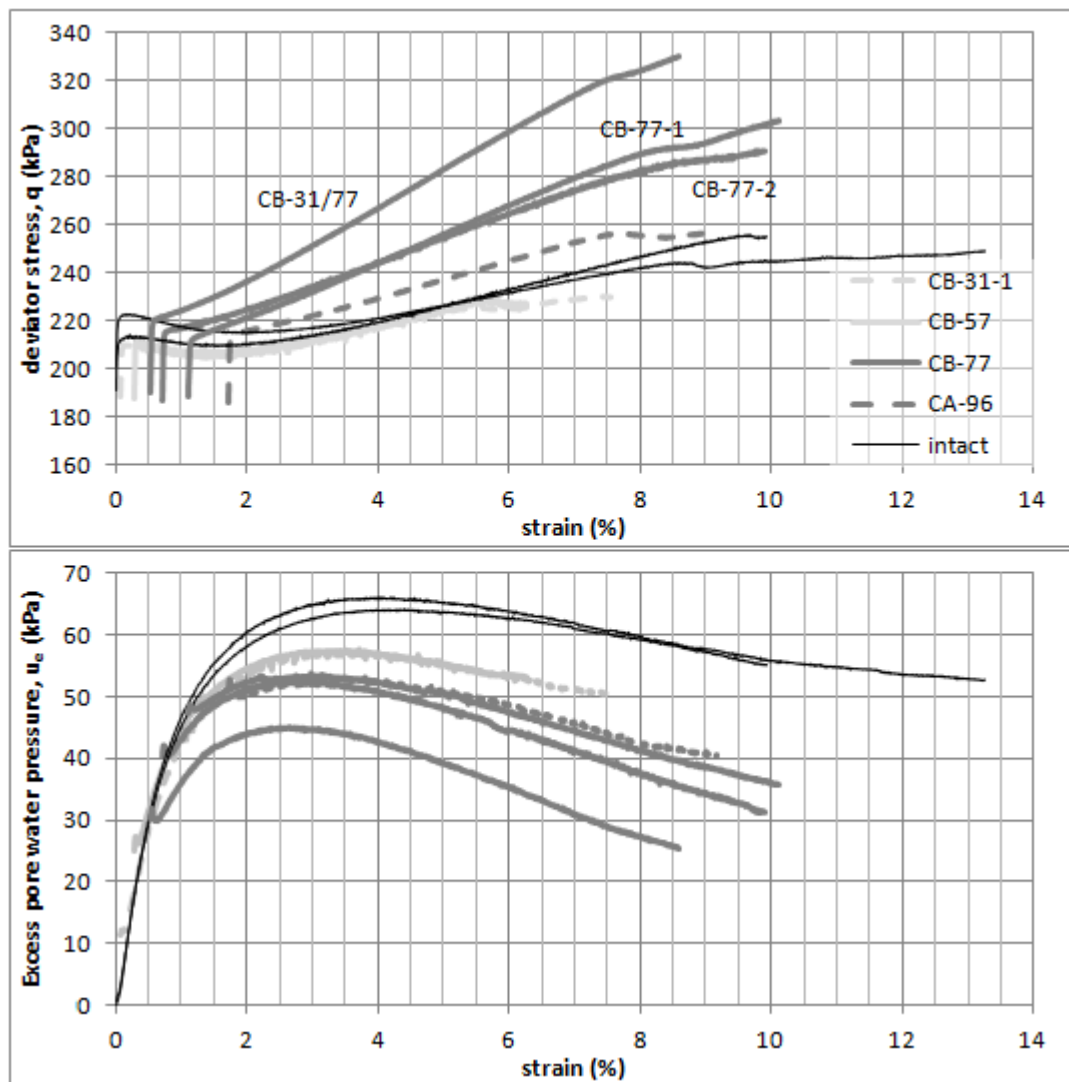
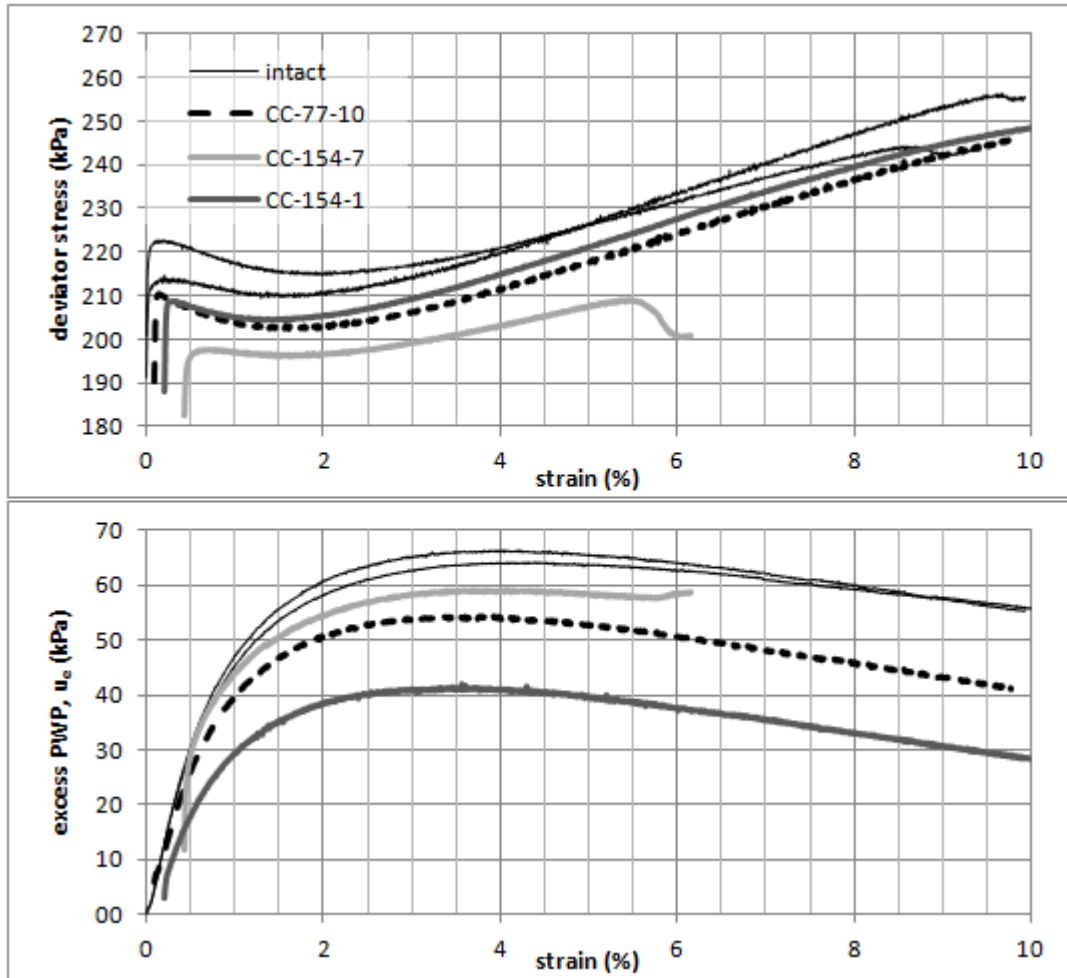


Figure 16: Post-cyclic monotonic shear response of cyclically liquefied Series 'A' tests with varying accumulated cyclic strain (final cumulative cyclic strain is the starting strain for post-cyclic curves); pore water pressure and deviator stress of cycled samples converge to the intact curve but can trigger shear banding at lower strengths, particularly with standard sample ends.



820

821 Figure 17: Post-cyclic monotonic shear response of samples not liquefying under cyclic load. N.b. CB-
 822 77-1 and 2 were conducted with different final consolidation creep rates (see Figure 7) to CB-31/77.



823

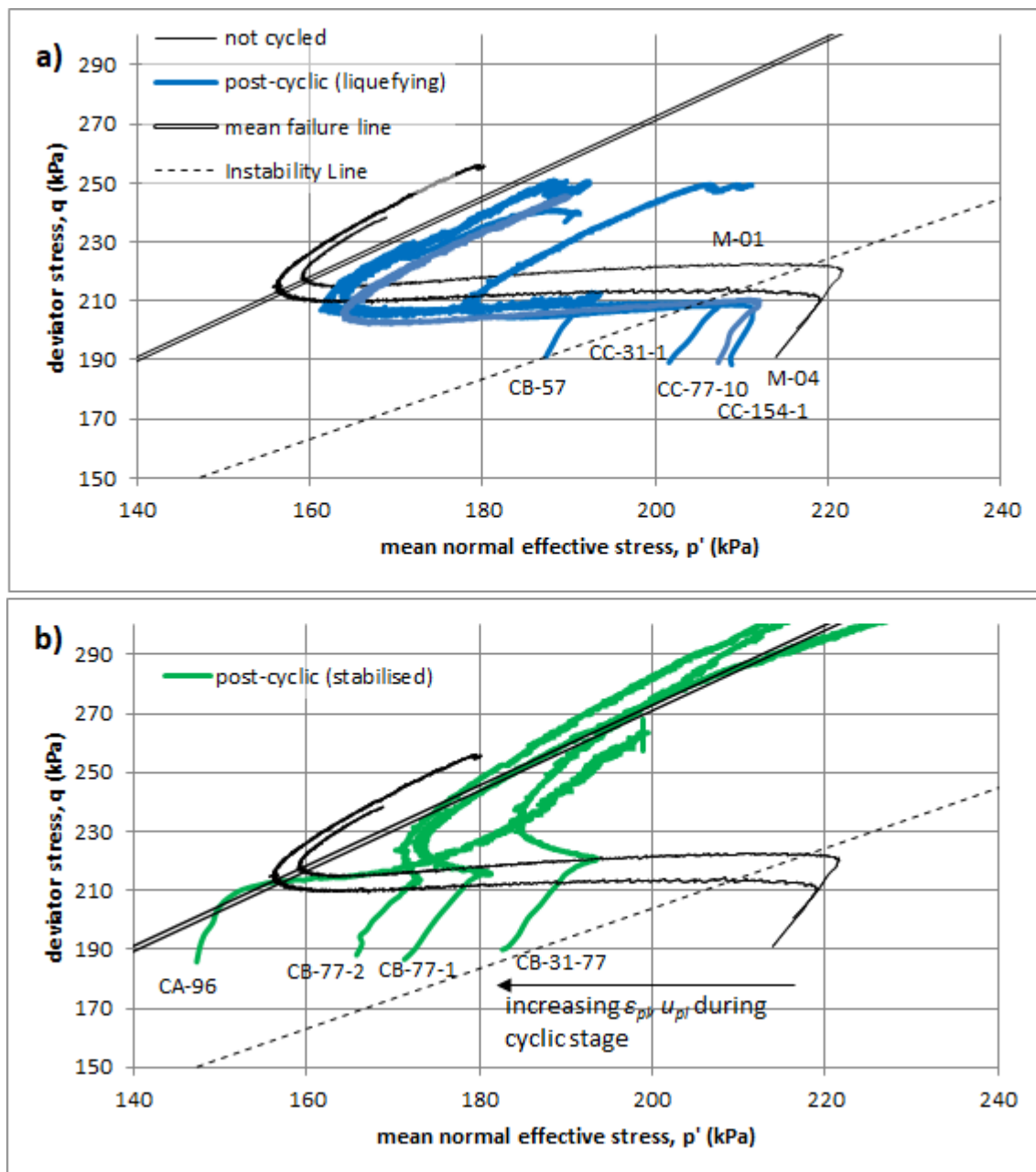
824

825

826

827

Figure 18: Monotonic post-cyclic Series 'C' tests: liquefaction behaviour retained for sub-threshold cycling ($\Delta q_{cyc} = 20\text{kPa}$; CC-77-10) terminated before exceeding liquefaction initiation strain (i.e. at 0.095%). and above-threshold cyclic stress (CC-154-1 and CC-154-7) either halted before liquefaction initiation (at 0.20%) or after (at 0.43%).



828

829 Figure 19: Undrained effective stress paths of post-cyclic monotonic tests with reference to the
 830 Instability Line and monotonic tests not subject to cyclic load. Similarly to Figure 12, the Instability
 831 Line separates liquefying (a) and stabilised (b) states for undrained monotonic shear.

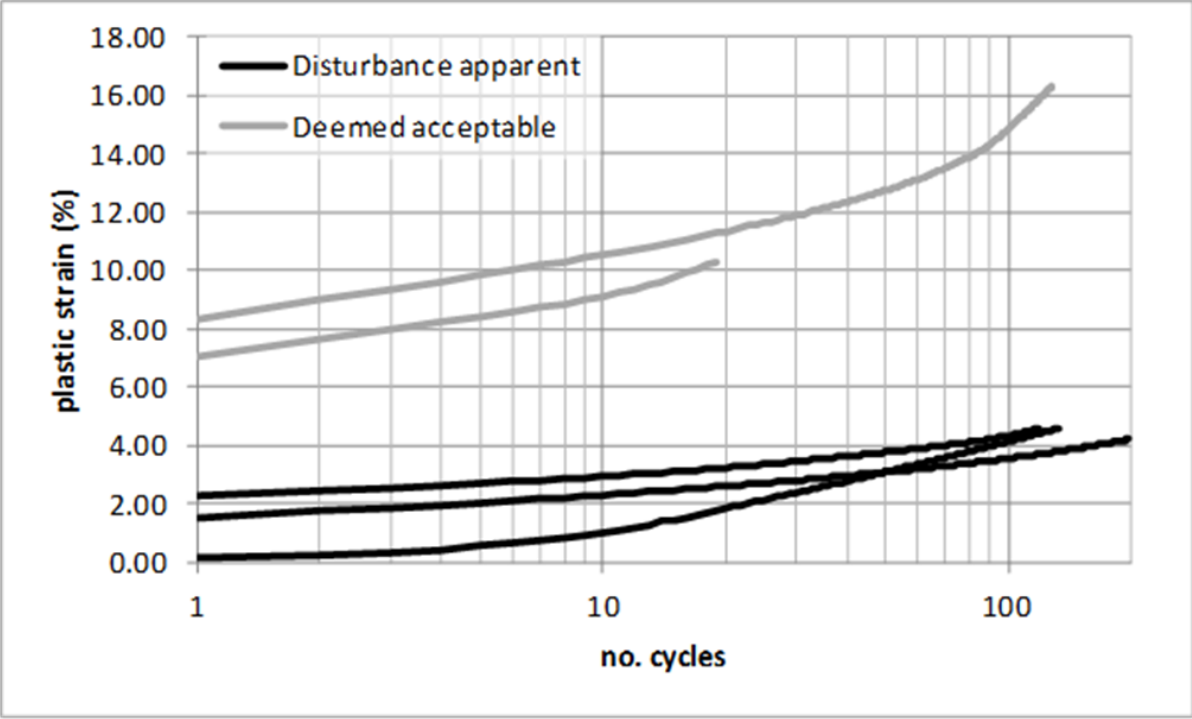


Figure 20: Reduced first cycle strain and ongoing accumulation as a result of sample disturbance prior to consolidation (CA-192 tests).